EVALUATING 1 AND 2D DEMINSIONAL MODELS FOR FLOODPLAIN INUNDATION MAPPING

by

M G ANDERSON AND P D BATES

FINAL TECHNICAL REPORT

[0012]

February 2002

United States Army

European Research Office of the US Army
London, England

CONTRACT NUMBER N68171-98-M-5830

Professor M G Anderson

REPORT DOCUMENTATION PAGE	Form Approved OMB No 0704-0188

Send comments regarding this burden estimate or any other aspect, including suggestions for reducing this burden to Washington Headquarters Services, Directorate for information Operations and Report, 1215 Jefferson highway, Suite 1204 Arlington, VA2202-4302, and to the Office of Management and Budget, Paperwork Reduction Project (0704-0188), Washington DC 20503

1. AGENCY USE ONLY (Leave blank)	2. REPORT DATE February 2002	3. REPORT TYPE AND DATES COVERED Final Technical report September 1998-December 2001

4. TITLE AND SUBTITLE Evaluating 1 & 2 dimensional models for floodplain inundation mapping	5. FUNDING NUMBERS N68171-98-M-5830

6. AUTHOR(S) Malcolm G Anderson Paul D Bates

7. PERFORMING ORGANISATION NAME(S) AND ADDRESS(ES) University of Bristol Department of Geography Bristol BS8 1SS UK	8. PERFORMING ORGANISATION REPORT NUMBER
9. SPONSORING/MONITORING AGENCY NAMES(S) AND ADDRESS(ES) European Research office, US Corps Engineers, London, England	10. SPONSORING/MONITORING AGENCY REPORT NUMBER

11. SUPPLEMENTARY NOTES

12a. DISTRIBUTION/AVAILABILITY STATEMENT	12b. DISTRIBUTION CODE

13. ABSTRACT (Maximum 200 words)

This project has sought to develop a suite of computational hydraulic models for high resolution flow prediction at the reach scale (10-60km) that directly addresses potential Corps of Engineers Research and Development agendas. Specifically, we have:

Developed a suite of models of varying complexity for long reach, high-resolution river flow prediction.

Developed through GIS technologies the integration to remote sensing data sets capable of parameterizing such models and examined data assimilation, redundancy and scaling issues.

Developed novel means of validating hydraulic models using newly available data sets from satellite and airborne sensing platforms.

Future opportunity: With the further advance of remote sensing technologies and high performance computing considerable potential now exists for computational hydraulic modelling at all scales up to and including the basin scale (100's of km). This has the potential to allow extension of the modelling techniques described in this report into the areas of: *Forecasting(*Real time forecasting, linkages to remote sensing driven snow-melt forecasting models, hydraulic impacts of climate and land use change), *Design(*soft engineering design in respect of land use, habitat specifications, development of maintenance schedules and impact assessments) *Management* (linking hydrologic and hydraulic models for Integrated Basin Management, floodplain management and planning, including integration of model outputs with socio-economic data sets to identify at risk populations, wetland restoration and management)

14. SUBJECT ITEMS	15. NUMBER OF PAGES 58
	16. PRICE CODE

17. SECURITY CLASSIFICATION OF REPORT	18. SECURITY CLASSIFICATION OF THIS PAGE	19. SECURITY CLASSIFICATION OF ABSTRACT	20. LIMITATION OF ABSTRACT
Unclassified	Unclassified	Unclassified	

Standard form 298 (Rev 2-89
Prescribed by ANSI Ltd Z19-18
298-102

EVALUATING 1 AND 2 DIMENSIONAL MODELS FOR FLOODPLAIN INUNDATION

CONTRACT N68171-98-M-5830

1. Introduction

1.1 Objectives of the study

- ***To produce a state of the art numerical model of a large reach of the Missouri River, capable of simulating high resolution spatially/temporally distributed results of water depth and velocity (TELEMAC 2D modelling system)***
- ***To investigate model behaviour through a sensitivity analysis.***
- ***To compare model predictions to multiple types of measured data, internal to the model domain, in order to assess model performance and the utility of the LANDSAT remote sensing validation data.***
- ***To develop a model application using LISFLOOD-FP employing SAR remote sensing data on a reach with high resolution data availability***
- ***To investigate the impact of varying levels of bathymetric data and mesh resolutions on the LISFLOOD-FP model predictions.***
- ***To assess the current R&D needs and opportunities in eco-hydraulics***

1.2 Background Information

The research in this contract focuses on achieving improved modelling and validation strategies for river flood inundation and the within-channel representation of flow processes. This style of research and investigation is of considerable importance for applications such as ensuring appropriate riverine habitat specifications, eco-hydraulics and river restoration issues.

To achieve these goals the research programme was structured in the following terms:

1. Background and key features of the study
2. Outline of the TELEMAC 2D modelling system for river hydraulic modelling
3. The Missouri River model: Bathemetric resolution and sensitivity of TELEMAC
4. The Missouri River model: Validating TELEMAC utilising LANDSAT TM data
5. Outline of the LISFLOOD model as a comparator model for river inundation and within channel flow process
6. Application of LISFLOOD using SAR remotely sensed data for validation purposes
7 Future R&D opportunities

1.3 Key Features of the study

- ***The application of a state of the art two-dimensional finite element code for modelling large scale fluvial hydraulics on the Missouri River.***
- ***The use of a high resolution model, in both space and time, along with wetting and drying algorithms for representing moving flow field boundaries allows dynamic inundation predictions.***
- ***For the first time model predictions are validated on this scale in both time and space using multiple data sources. The data sources are internal stage data at two sites, supplied by the USACE Missouri River District (MRD), and satellite imagery, supplied by the Remote Sensing and Geographic Information Systems Center at USACE Cold Regions Research and Engineering Laboratory (CRREL).***
- ***The strength of model validation is graded depending on the data source and model prediction.***
- ***The influence of bathymetric data on the model predictions is studied for its potential in aiding future data collection strategy.***

2. Outline of the TELEMAC 2D modelling system for hydraulic modelling

The TELEMAC system has been developed by the Départment Laboratoire National d'Hydraulique (LNH) at Electricité de France, Direction des Études et Recherches (EDF-DER). LNH was formed in 1946 to undertake studies for EDF's hydroelectric power projects and to solve the hydraulic engineering problems of the Maritime Ports and Waterways Authority. Since 1965 the role of LNH has changed somewhat. About 70% of LNH's work is now directly for the benefit of EDF, split between hydraulics inside power station machinery and the study of environmental problems in rivers, seas and the atmosphere brought about through the siting of such plants. The rest of LNH's work is on behalf of other organisations.

The TELEMAC system therefore follows a line of hydraulic simulation codes originating from LNH for the study of environmental problems, such as flooding resulting from a dam break or thermal emission into a river or estuary. TELEMAC was developed from the ULYSSE code, a 2D finite difference system (Ulysses being the father of Telemachus in Greek mythology). TELEMAC is now in its third four year development period, each period having a budget of circa US$16 million (Hardy, 1997). TELEMAC is a general purpose code that is applicable to many situations beyond the original remit of its design, such as natural floods on rivers.

The TELEMAC system is a series of computer programs utilising finite element techniques for simulating hydraulic situations. The system includes pre- and post-processing components and offers solutions in two- and three-dimensions. It also contains facilities for sediment and contaminant transport (SUBIEF) and sand transport (TSEF). The full system is further outlined in Figure 2.1. All the components of the system have common file formats and are written in the high level language FORTRAN 90. This enables easy file transfer between components of the system and allows model users to modify parts of the code as desired for specific applications.

The TELEMAC system contains both two- and three-dimensional versions. The three-dimensional version (TELEMAC-3D) has advantages in many applications where vertical velocity variations are important such as small scale and oceanic studies but in large scale fluvial applications depth averaged calculations are adequate. Indeed the equations used in nearly all fluvial hydraulic models derive from the depth averaged equations known as the Shallow Water or St. Venant Equations, TELEMAC-2D being no exception. The third dimension, though initially appealing, would simply add to the computational and data demands. Descriptions of TELEMAC-3D can be found in Hervouet *et al.* (1994), Hervouet and Janin (1994) and Hervouet and Van Haren (1996). TELEMAC-2D is however used throughout the work presented here and is now discussed in more detail.

2.1 TELEMAC-2D

The main features of TELEMAC-2D are listed by Hervouet *et al.* (1994) as:

- structured or non structured meshing,
- use of Cartesian or spherical co-ordinates,
- subcritical and supercritical regimes (with hydraulic jumps),
- various momentum source terms : bottom friction, wind stress atmospheric pressure, Coriolis force,
- turbulence modelling (zero equation model, k-epsilon model),
- equation on temperature or a substance concentration,
- treatment of tidal flats,
- many types of boundary conditions including free slip condition and incident waves.

Many of these are of minimal importance for fluvial applications but are necessary for the diverse nature of cases that TELEMAC-2D can be applied to. A wide range of test cases are illustrated in the TELEMAC-2D (version 3.0) validation document (Cooper, 1996) prepared to substantiate the explicit claims made about the applicability and accuracy of the computer code. The test cases illustrated range from the Western European Coast and the Mersey estuary UK, to flows around bridge piers and over a weir. On a scale more relevant to this study dam breaks, flow at a river confluence and the simulation of a flood event on the River Culm, UK are also shown. A new version of TELEMAC-2D is released annually. All of the simulation in this report have been carried out using version 3.0, released in 1995.

2.1.1 Shallow water equations

TELEMAC-2D solves the shallow water equations (SWE), the depth averaged version of the fully three dimensional Navier Stokes equations of fluid flow. The SWE require that:

- the flow is incompressible
- the water column is well mixed, so that there are no significant density variations in the vertical
- vertical accelerations are negligible (hydrostatic pressure approximation)
- the effective turbulent stresses can be represented by an eddy viscosity concept (the Boussinesq assumption)
- bed stresses can be modelled using a linear or quadratic friction law.

All of these conditions are commonly met in rivers, estuaries and seas making the choice of these equations over the full three dimensional Navier-Stokes equations valid for the applications of the model (Cooper, 1996).

The choice of formulation of the SWE used in TELEMAC-2D is not obvious. A conservative form would seem better but divisions by the water depth are needed to produce the velocity field, hence causing problems in dry areas of the model domain. Hence a non-conservative form is preferred. Moreover numerical stability analysis also favours the non-conservative version of the equations. Using finite element methods mass conservation can be ensured with non-conservative equations. Two versions of these non-conservative equations have been developed, the celerity-

velocity version and the depth-velocity version. The depth-velocity version are marginally favoured as they have better mass-conservation properties (Hervouet and Janin, 1994). These equations are shown below:

$$\frac{\partial h}{\partial t} + \mathbf{u}.\mathbf{grad}(h) + h.\mathrm{div}(\mathbf{u}) = 0 \qquad 2.1$$

$$\frac{\partial u}{\partial t} + \mathbf{u}.\mathbf{grad}(u) + g\frac{\partial h}{\partial x} - \mathrm{div}(v.\mathbf{grad}(u)) = S_x - g\frac{\partial Zf}{\partial x} \qquad 2.2$$

$$\frac{\partial v}{\partial t} + \mathbf{u}.\mathbf{grad}(u) + g\frac{\partial h}{\partial y} - \mathrm{div}(v.\mathbf{grad}(v)) = S_y - g\frac{\partial Zf}{\partial y} \qquad 2.3$$

where:

h : water depth

u, v : velocity components

g : gravity

Zf : bottom elevation.

Sx, Sy :Source/sink terms (bottom friction, wind, etc.)

ν : eddy viscosity

h, u & v are the unknown variables.

Equation 2.1 being the continuity equation, 2.2 and 2.3 the force-momentum equations. Full derivations can be found in Norton *et al.* (1973).

2.1.2 Solving the equations

The TELEMAC system uses a finite element methodology to solve the shallow water equations to produce values of water depth (h) and two velocity components (u and v) at all points in the model domain. To achieve this the domain must be discretized into a grid or mesh, usually made up of linear triangles (unstructured grid) for flexibility. The mesh is created outside TELEMAC using specialised mesh generation software such as I-DEAS or BALMAT. The mesh is then incorporated with the topographic data to produce a geometry file that is then used in the TELEMAC-2D simulation. The mesh consists of a series of node points, the vertices of the triangles with a elevation (z) value, where the equations are solved and the triangles themselves are the elements. The geometry notation used is shown in Figure 2.1.

All three dependant variables (h,u and v) are defined at each point in the domain in terms of linear interpolation functions associated with the value attained at each node. Linear interpolation functions between nodes can be a limitation where the bed gradients are varying rapidly compared to the distance between nodes. Mesh refinement can however be used to overcome this problem in most cases. The time discretization is semi-implicit so a system of 3N simultaneous algebraic equations is obtained, where N is the number of nodes in the domain (Cooper, 1996). Furthermore, TELEMAC-2D employs element by element (EBE) techniques to minimise and

simplify computation. More detailed descriptions of finite element methodology can be found in Norton *et al.* (1973) and Pinder and Gray (1977).

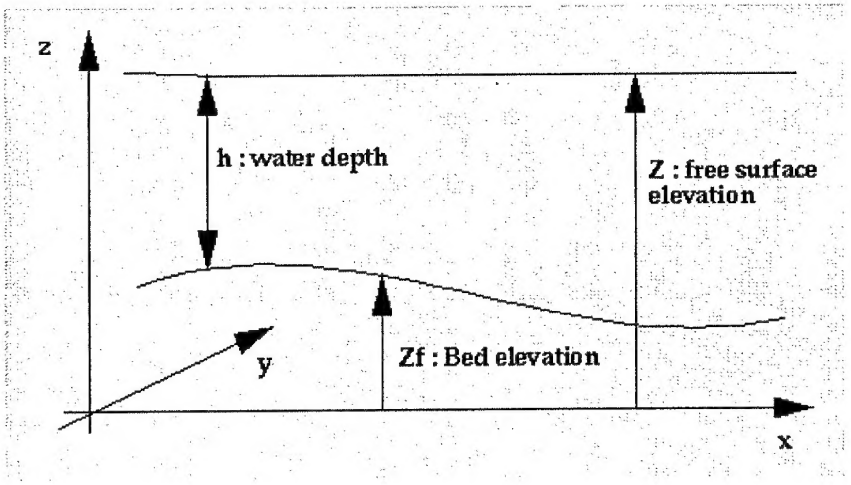

Figure 2-1 The geometry notation used in TELEMAC-2D (after Hervouet and Van Haren, 1995).

Several solution algorithms are available in TELEMAC-2D including (Cooper, 1996):

- a fractional step method using characteristics for the advection terms and a Galerkin method for the propagation and diffusion terms in the equations
- several variants of the Streamline Upwind Petrov Galerkin (SUPG) method (Brooks and Hughes, 1982)
- a hybrid scheme that combines the characteristics and SUPG approaches.

Further details of these options are available in Hervouet and Van Haren (1995).

In the simulations presented later in this report a fractional step method (Marchuk, 1975) is used where the advection terms are solved initially followed by a second step where the propagation, diffusion and source terms are solved. For the advection step the Method of Characteristics is used for the momentum equation and an SUPG method for advection of h in the continuity equation, ensuring mass conservation. The use of the semi-implicit SUPG method for the continuity equation achieves unconditional stability (Hervouet and Janin, 1994). The second step of the calculation, propagation, is then solved using a conjugate gradient type method.

The different solution techniques do however produce very similar results when used on the same simulations with the same mesh. For example Bates *et al.* (1996) show the SUPG and hybrid methods used on a flood event on the River Culm, UK, showing very similar outflow hydrographs and inundation extent.

The Courant number is used as a measure of the quality of the numerical solution. It derives from explicit numerical methods and is calculated thus:

$$C_r = u\frac{\Delta t}{\Delta x} \qquad 2.4$$

where (Bates *et al.* 1996):
C_r : Courant number
t : time step
x : mesh size
u : flow velocity.

Explicit methods become unstable when C_r>1. Although TELEMAC-2D is implicit and theoretically not subject to such constraints the Courant number remains a good measure of the quality of the numerical solution (Hervouet and Janin, 1994; Bates *et al.*,1996). Hervouet and Janin (1994) suggest that in some cases simulations can be performed with values of the Courant number of up to 50 but this is not advisable.

2.1.3 Boundary conditions

There are two main types of boundary condition that can be used, solid boundaries and liquid boundaries. The boundaries described here are round the sides of the model domain and through the bed of the model. All boundary conditions are assigned on a node by node basis. Solid boundaries are no flux (impermeable) and incorporate a friction factor (Hervouet and Van Haren, 1995). Liquid boundaries allow a flux across them. They are more difficult to deal with as they suppose the existence of a fluid area that is not part of the calculation domain but can however influence it. This influence is described through the boundary condition. There are four types of liquid boundary, entry and exit with supercritical flow (Froude number >1) and entry and exit with subcritical flow (Froude number<1). Incident waves and prescribed flowrates can be incorporated through these 4 boundary types. Hervouet and Van Haren (1995) describe these boundary conditions more fully.

2.1.4 Physical parameter options

Physical representation of parameters is essential in models such as TELEMAC-2D in order to apply them to different applications. TELEMAC-2D includes numerous physical parameters. The most important are discussed in this section.

2.1.4.1 Bottom friction

There are six options in TELEMAC-2D for representing bed friction, these are:
- No friction
- Linear friction
- Chezy's law
- Strickler's law
- Manning's law
- Nikuradse's law

The applied friction coefficient is converted to force terms in the x and y directions at each computational node which are then fed into the Shallow Water Equations (in the source terms Sx and Sy - see section 2.1.1., equations 2.2 and 2.3). In reality the bed friction force is a quadratic function of velocity so the no friction and linear law are rarely used in practical applications (Hervouet and Van Haren, 1996). The Chezy, Strickler and Manning laws are all closely related and utilise the quadratic function mentioned and are all described more fully by Hervouet and Van Haren (1995). Nikuradse's law calculates a Chezy coefficient from the water depth (h) and grain size of the bed material which is then converted into a force term. Choice of law is not critical as they are very closely related and friction coefficients can easily be converted between them. The choice rests with the model user.

2.1.4.2 Turbulence representation

Turbulence is one of the major unresolved problems in physics. Its importance in hydraulics is well known but it's representation in hydraulic models is a different problem. The concern in hydraulic modelling is how turbulence in flow affects the mean structure of the flow. Turbulence modelling is a scientific discipline in itself and the reader is referred to Younis (1996) for a general discussion of turbulence modelling and to Hervouet and Van Haren (1996) for a fuller exposition of turbulence representation in TELEMAC-2D than is possible here. In TELEMAC-2D version 3.0 there are two options for turbulence representation:

- constant viscosity
- k-epsilon model.

The first and simplest is a constant viscosity coefficient, zero-equation turbulence model. The term VELOCITY DIFFUSIVITY is used to set the molecular viscosity, turbulent viscosity and dispersion throughout the model domain. In turbulent flows the turbulent viscosity is dominant and can virtually be equated to the velocity diffusivity value. A constant value of turbulent viscosity over the model domain is often used but is an oversimplification.

The second available closure is the k-epsilon model where the turbulent viscosity is expressed as a function of the turbulent kinetic energy (k) and its dissipation rate (ε). This two-equation turbulence model is overcomplicated for large scale applications and is computationally intensive.

A third turbulence model, the single-equation Elder's model, has just been introduced into the newest version of TELEMAC-2D (version 3.1). This model separates longitudinal and transverse dispersion terms. It offers improvements on the previous two methods in fluvial applications where such separation is important. Unfortunately this method was not available for the work in this report.

2.1.4.3 Other physical parameters

Several other physical parameters can also be specified in TELEMAC-2D. These include wind stress on the water surface, atmospheric pressure, water temperature and water density. The Coriolis force can also be applied when modelling large areas.

2.1.5 Wetting and drying zones

Applications of TELEMAC-2D to rivers and estuaries generally involve wetting and drying of areas of the model domain. For example the tidal simulation in the Mersey estuary and the flood event on the River Culm, both described by Cooper (1996), involve this type of behaviour. The ability of the model to deal with this sort of behaviour is therefore of vital importance but is problematic. The behaviour in the dry zones, where divisions by the water depth (h) in the calculations, can cause spurious terms to appear as h tends towards zero.

Two solutions to this problem are available in TELEMAC-2D, both described in more detail by Hervouet and Van Haren (1995),

- solving the equations everywhere and coping with the spurious terms.
- removing the dry zones from the computational domain.

The first is the simplest but corrections must be applied in the dry zone. In dry areas the water surface gradient becomes that of the bottom topography but this cannot be allowed to act as a driving force in the momentum equation.

The second method removes the dry zone from the computational domain and is often called the "moving boundary technique". In TELEMAC-2D this is achieved efficiently, avoiding the need to redefine the mesh at each time step, by keeping the elements in the mesh but cancelling their existence through the use of an array set to 0 for dry elements and 1 for all others.

Partially dry elements are another important area, especially where the elements are large such as in the Missouri River model. These are coped with in TELEMAC-2D by a sophisticated method that allows the water depth to go to zero within an element. This compares favourably with the usual techniques of keeping the elements fully wet or excluding partially dry elements (Figure 2.2).

2.2 Post-processing of results

After the computations have been completed the numerical results must be converted to a more user friendly visual form. This is done using the graphics visualisation software RUBENS, also written by EDF-DER. RUBENS allows quick, easy and flexible representation of the results in many different forms such as:

- mesh plots
- vector fields
- contour lines
- coloured surfaces
- space profiles
- time profiles

RUBENS also allows the superposition of measurements and graphics and also the manipulation and processing of the visualised data. Most of the plots of model results in this report are created using the RUBENS software. For more information on RUBENS the reader is referred to Piro (1993).

2.3 Summary of the TELEMAC-2D system

TELEMAC-2D is a high resolution space/time distributed hydraulic model that solves the Shallow Water Equations for fluid flow using a finite element methodology. The model can be used in a wide variety of scenarios including those involving wetting and drying fronts within the model domain. Bed friction and turbulence are represented in the model through the use of physically based parameters.

TELEMAC-2D can therefore be seen to be well specified for the type of fluvial application that is of interest in this study. The code has been shown to work, through the report of Cooper (1996), in a wide range of cases. Success in any individual situation is however dependant on the data provided, physical and numerical parameters used. How these important factors have been determined in the Missouri River model case is the subject of the next section

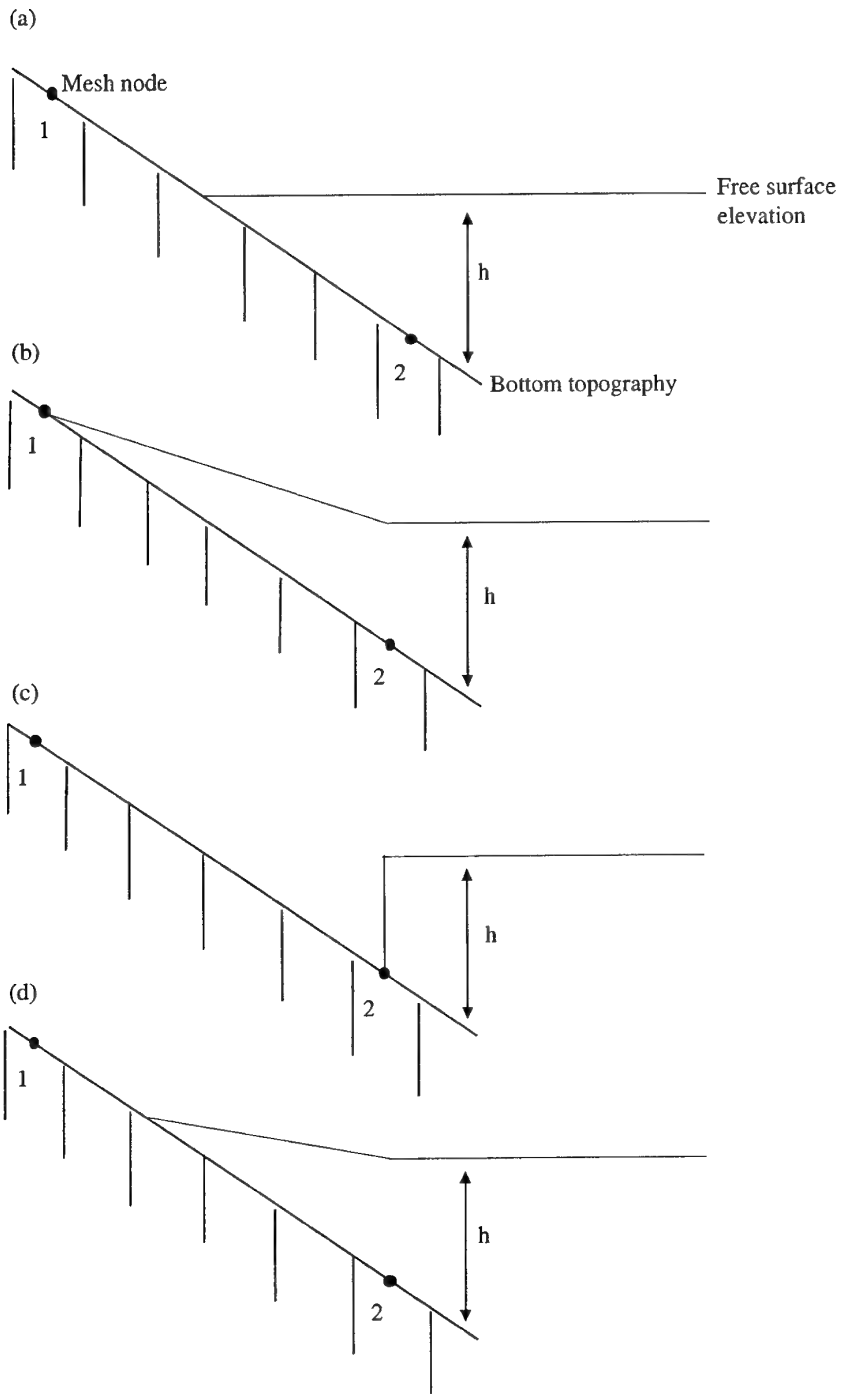

Figure 2-2 Partially dry elements: (a) the real situation, (b) element remaining fully wet introducing spurious momentum terms, (c) element exclusion method and (d) TELEMAC-2D method keeping the element partially dry (after Price, 1997).

3. The Missouri River model : Bathemetric resolution and sensitivity of TELEMAC

This section looks at how TELEMAC-2D has been applied to the Missouri River between Gavins Point Dam, South Dakota, and Maskell, Nebraska. The theoretical aspects of the model were examined in section 2 but the practical details of applying the model to this specific scenario reach are vital to gain an understanding of the model and its capabilities.

The reach of the Missouri River being used for this modelling study is that from Gavins Point Dam, South Dakota, to the gauging station at Maskell, Nebraska (Figure 3.1). The reach covers river miles 811 to 776 making it 35 miles or 55 km long. The channel varies in width between 300m and 1200m. The channel slope is very low, dropping only about 12 metres along its 55 km length, giving a gradient of 0.02%. The bed material in this channel is sand which is fairly mobile but the channel banks have been strengthened or stabilised along much of the reach. There are several islands along the reach several of which are permanent. There is one major tributary, the James River, that joins the main stem at river mile 800 adjacent to the James River Island.

The flow out of Gavins Point Dam is regulated to minimise the risk of flooding downstream, hence the reach being modelled is very unlikely to attain an out of bank conditions. The flow in the James River is, however, naturally variable. The model of this system can therefore remain as channel only. River flow data is available at several points along the reach on an hourly basis. Table 3.1 shows the data availability and gauge locations (also Figure 3.1).

Table 3-1 Gauge station location and data availability.

Gauging Station	Distance from top of reach (km)	Data Available
Gavins Point Dam, SD.	0	Flow rate
Yankton, SD.	7.5	Flow rate and Stage
Gayville, SD.	21.5	Stage
Maskell, Neb.	55	Stage
Scotland, SD.	53 km up James River from confluence	Flow rate and Stage

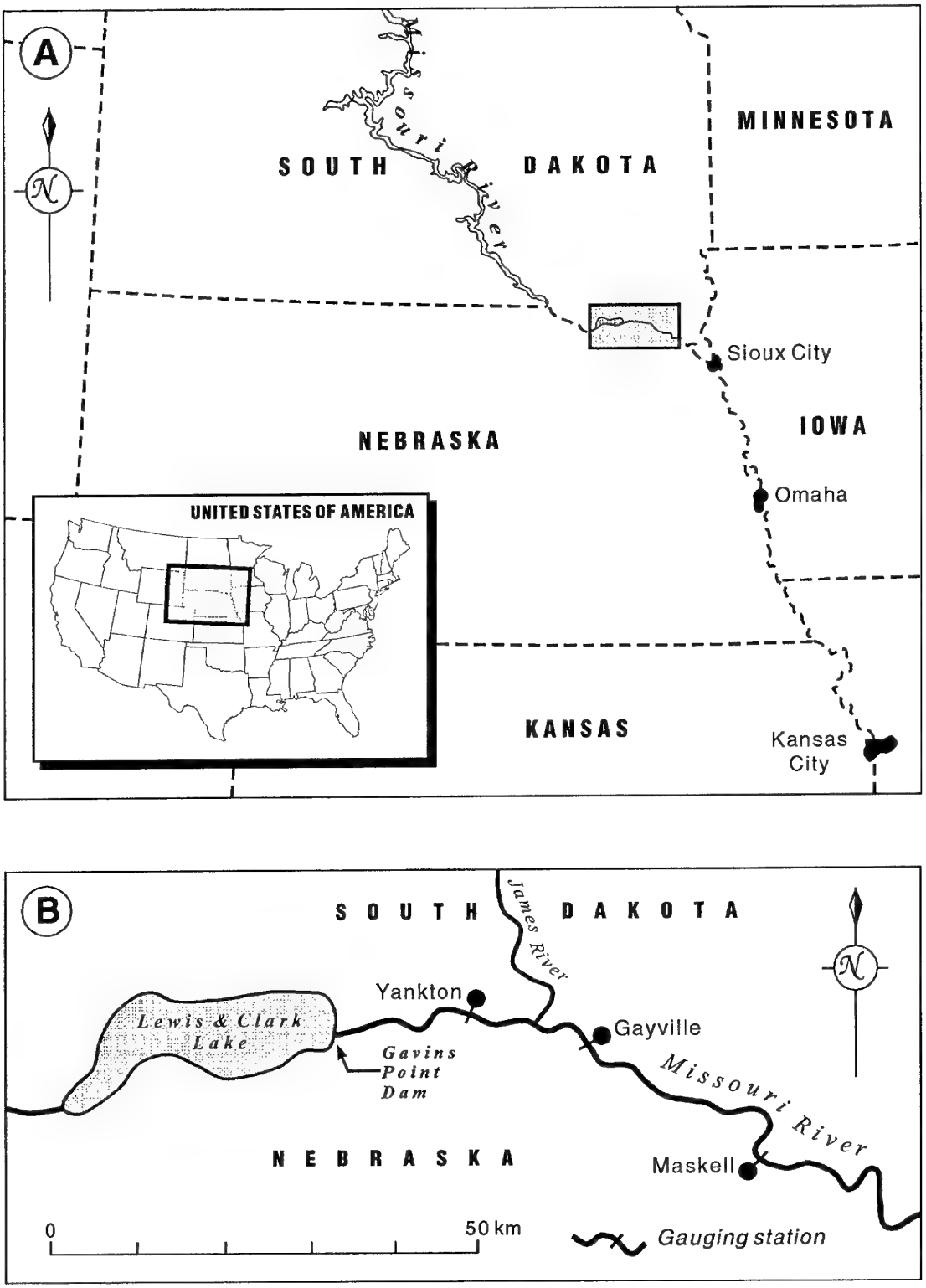

Figure 3-1a) Location and (b) detail of the study reach of the Missouri River, USA. The modelled reach is from Gavins Point Dam to Maskell and includes the gauging stations at Yankton and Gayville.

The flow from the James River gauge at Scotland, South Dakota, is routed using a simple one-dimensional kinematic wave model to the required location on the main model input boundary when necessary.

The hydraulic model used in this study is TELEMAC-2D. This is a high resolution space/time distributed hydraulic model using the finite element methodology. The model is potentially capable of fulfilling all the objectives of this study. The model is described in detail in section 2.

3.1 Producing the finite element mesh

The finite element mesh for the model must be created by first defining the boundary of the model domain and secondly discretizing this area into elements.

The boundary of the 2D model was defined by digitising round the edge of the river as represented on United States Department of the Interior 7.5 minute quadrangle series maps. The use of wetting and drying algorithms in the model enable the flow field boundary to be calculated within this outer boundary thus allowing this boundary to be fairly loosely defined. The digitised boundary was then converted to Universal Transverse Mercator (UTM) metre co-ordinates for compatibility with the metric scale used by TELEMAC-2D. The boundary of the model (with TELEMAC-2D's metric scale), which includes three permanent islands, is shown in Figure 3.2.

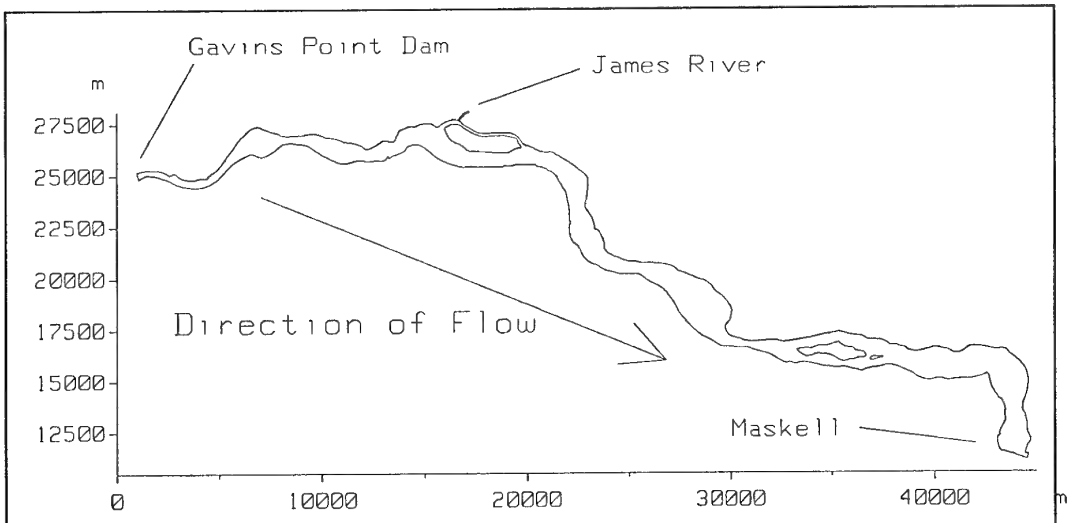

Figure 3-2 The boundary delineation of the Missouri River model.

A mesh of triangles or quadrilaterals must be made within the model domain to facilitate the finite element solution technique. The finite element meshes used with the Missouri model were generated inside the prescribed boundary using the mesh generation package BALMAT. The meshes created were made of near equilateral triangles in order to increase the accuracy and minimise mass conservation errors.

Two meshes have been created of this reach. The two are shown in Figure 3.3 and their attributes compared in Table 3.2.

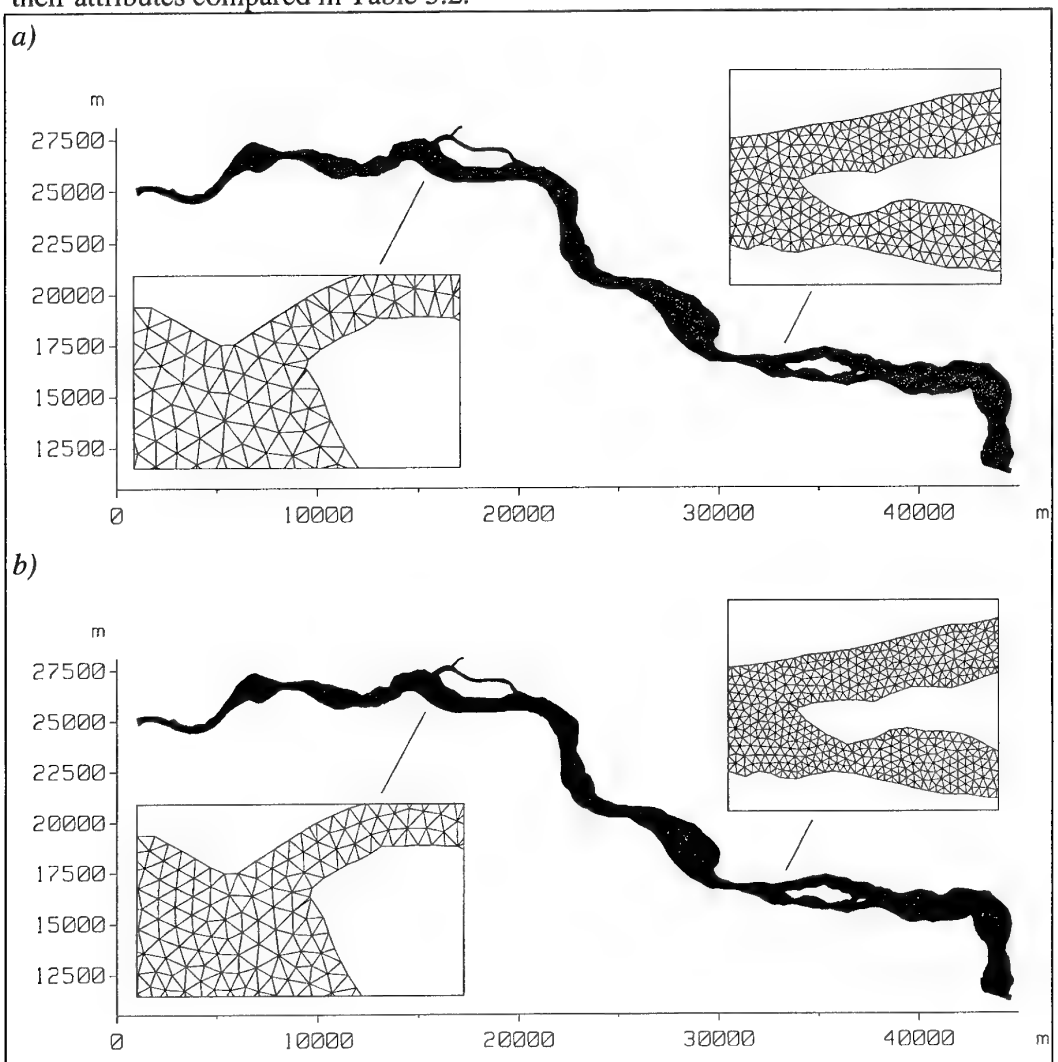

Figure 3-3 Finite element meshes of the Missouri River from Gavins Point Dam to Maskell, (a) low resolution Mesh 1 and (b) high resolution Mesh 2.

Mesh 1, the lower resolution mesh, is used for the majority of the simulations in this report. It should be assumed this has been used when looking at results unless otherwise stated. Mesh 2 is only used in the sensitivity analysis (section 4) and section 6 where its performance is compared to that of mesh 1.

Table 3-2 Comparison of the attributes of the two meshes used to model the Missouri River in this report.

Attribute	Mesh 1	Mesh 2
Number of Nodes	5969	9213
Number of Elements	10437	16567
Average Element Size (m^2)	100.77	79.98

3.2 Bathymetric Data

The bathymetric data in a 2D hydraulic model is one of the most important factors in attaining high quality simulations. The quantity and quality of the bathymetric data is therefore of utmost significance.

Along this reach of the Missouri River the bathymetry was obtained by the MRD in 1995 by echo sounder surveys of channel cross sections. In total 343 cross sections were available along the 55 km reach creating an average spacing of just over 150m. Each cross section was made up of between 30 and 200 data points, depending on section length. The typical spacing between data points along a section was 6m. All elevation data were converted to metres. Bathymetric data were missing on the cross sections where the bed was above the water surface, such as on sand banks and mud flats. In these regions the topographic elevation was estimated from United States Department of the Interior 7.5 minute quadrangle maps, except on the permanent island in the model where no such data is required.

The bathymetric data must now be applied to the finite element mesh. This is the process of interpolating between topographic data points and assigning elevation (z) values to the nodal points in the mesh. This produces a geometry file for the model simulation. The interpolation is usually carried out using STBTEL, the TELEMAC sub-program. This uses a quad-directional interpolation routine, taking the nearest data point in the four quadrants around each node, weighting for distance from the node and combining to give the nodal elevation. An alternative interpolation routine has been written at Bristol for use with cross sectional data of river channels. This is a linear interpolation down the line of greatest depth between sections and improves the definition of this line in such cases as the Missouri River. A portion of the models topography is shown in Figure 3.4.

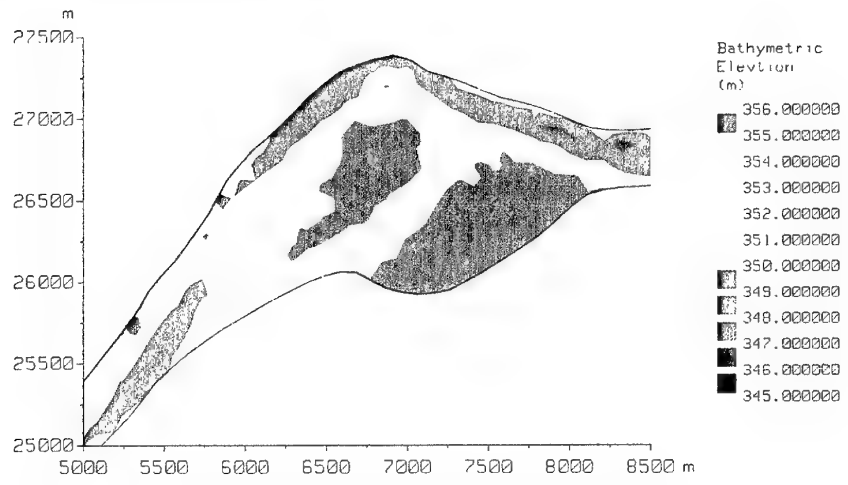

Figure 3-4 An example portion of the models bathymetric representation. This section is immeadiately upstream of Yankton.

3.3 Boundary Condition Specification

The boundary conditions of the model are very important to the simulations run. There are several boundaries to each model that must be set with care prior to the model run. These boundaries are divided into two types, liquid boundaries and solid boundaries.

With the Missouri model, the liquid boundaries, allowing flow across them, are at the top and bottom ends of the reach and on the James River tributary inflow. Model inflows are prescribed as flowrates, at Gavins Point Dam and from the James River, and outflows as water surface elevations, at Maskell. This produces a well posed problem for fluvial flows according to the theory of characteristics (Hervouet and Van Haren, 1995). All measured flowrates were converted to m^3/s (cumecs) and stage values to metres.

Solid boundaries allow no flux across them. They are found down the sides of the reach and at the bed. The side boundaries in the Missouri model are set as slip boundaries, allowing a velocity along them. This is justified by the size of the elements making flow overly restrained in areas of channel constriction when the more realistic no-slip boundaries are imposed. The flexible boundary of the flow field removes this problem for large portions of the reach where such an argument is irrelevant.

3.4 Physical Parameter Specification

The two most important physical parameters in fluvial hydraulic models are generally agreed to be bed friction and turbulence (Baird and Anderson, 1990; Bates *et al.*, 1992). The theory of the two in TELEMAC-2D has been discussed in Section 2. They are the only two considered in any detail here.

Given the channel only nature of the model and lack of additional information the bed friction and turbulence parameters were defined as constant throughout the entire reach. These are obviously simplifications but should be adequate as a first approximation. The bed friction is always defined using Manning's law enabling the standard Manning's 'n' measure of flow resistance to be used. The turbulence was defined using the zero-equation velocity diffusivity representation.

3.5 Sensitivity Analysis

The first stage in model application is the sensitivity analysis. Sensitivity analysis is a widely used technique in hydrological and hydraulic modelling to determine the impact of changing parameter values and/or input stresses on the model predictions. Virtually every modelling study involves a sensitivity analysis at some stage. It is a technique that is potentially useful in model formulation, model calibration and model verification (McCuen, 1973).

3.3.1 Background to the sensitivity analysis

Howes and Anderson (1988) suggest that a sensitivity analysis can be used to:

- Demonstrate that in response to representative variation of model input and parameter values, theoretically realistic model behaviour is experienced.
- Illustrate the model to be sufficiently sensitive to represent actual variation in the prototype system.
- Identify those model parameters or inputs to which the model is most sensitive.
- Assess model behaviour without recourse to comparisons to field data.

Perhaps more importantly in the case of this model is that sensitivity analysis is very useful for deciding which parameters to adjust during calibration. Adjusting the most sensitive parameters will produce a greater improvements in the predictions for small changes in parameter values, which means that if the initial values were approximately physically realistic then the calibrated ones should be as well. Conversely if the less important parameters are left fixed at incorrect values then the resulting error on model predictions is likely to be small (Troutman, 1985).

Some of the theoretical considerations of sensitivity analysis are now discussed. Sensitivity is defined as the rate of change in one factor with respect to change in another factor. Mathematically it can be derived from a Taylor series expansion of model behaviour and after discarding the non-linear terms the linearized sensitivity (S) can be expressed in simple terms as (McCuen, 1973)

$$S = \partial F_0 / \partial F_i \qquad 3.1$$

where F_0 the model output prediction and F_i is the model input parameter. In many instances this linear approximation of sensitivity is adequate to describe model behaviour but whether it is appropriate for the Missouri model is unknown at present.

There are two methods for determining the value of the model sensitivity which are (Lane *et al.*, 1994).

- The direct differentiation of the governing equations. This has been demonstrated with simple models, for example Beven (1979) uses this method to assess the sensitivity of the Penman-Monteith evapotranspiration equations and LaVenue *et al.* (1989) use it to help estimate travel time uncertainties in ground water flow. However with complex, distributed models this methodology has not been developed sufficiently and cannot possibly assess the entire complex response of a model such as TELEMAC-2D.
- Factor perturbation approaches can evaluate the sensitivity of the model by incrementing parameter values and assessing the model response. This is the most commonly used form of sensitivity analysis.

Given the problems of direct differentiation in assessing the sensitivity in complex models the factor perturbation approach is the only one considered in this rest of this section.

Assuming the overall physically based validity of TELEMAC-2D to this type of application the sensitivity analysis of the Missouri River model has one major function. This to set up the basis for the following calibration procedures by determining:

- the relative sensitivity of the different physical parameters,

- the effect of mesh resolution on this.

Once these questions have been resolved the application and calibration of the model can proceed.

The runs carried out in this sensitivity analysis are outlined in Table 3.3. The data from these simulations is enough to fulfil the two aims above. As discussed in the previous section only two physical parameters in the model were varied, bed friction and turbulence representation (velocity diffusivity), both of which were evenly distributed across the domain.

Table 3-3 The simulations carried out for the sensitivity analysis. The figures in bold are the parameter values held constant whilst the other is varied.

Parameter Varied	Mesh 1	Mesh 2
Bed Friction (n)	0.01, 0.015, 0.02, **0.025**, 0.03, 0.035, 0.04	0.01, 0.015, 0.02, **0.025**, 0.03, 0.035, 0.04
Turbulence (Velocity Diffusivity - m^2/s)	1, **2**, 4	1, **2**, 4

The range of bed friction was chosen to represent the very broad range for this channel type, sand-bed with a shallow gradient (0.02% in this case) (Table 3.4). This full range is used here as no data are available to make a further judgement at this stage and uncertainties in the overall model set-up create the possibility that the values needed to fit the results to the observed are not those that would be selected from the field. The velocity diffusivity values are harder to justify physically given their vastly oversimplified application to the flow. The values chosen are similar to those used in other applications that have performed well, producing realistic output and maintaining model stability.

Table 3-4 Values of Manning's n for various channel types (after Bathurst 1988).

Channel Type	Channel Slope (%)	Manning 'n' range
Sand-bed	<0.1	0.01 - 0.04
Gravel-bed	0.05 - 0.5	0.02 - 0.07
Boulder-bed	0.5 - 5	0.03 - 0.2
Steep pool/fall	>5	0.1 - 5

The parameter space was sampled using simple single parameter perturbation techniques. The flow record used for these sensitivity tests is that from around the 6th June 1994 when the river is essentially at a steady state. The results are therefore all steady state values of the variables.

3.5.2 Results of the sensitivity analysis

The results of the parameter changes are looked at on the inundated area, water depth at Gayville and Yankton, velocity at Gayville and the spatial distribution of

differences of water depth and velocity between two runs over the whole domain. At this stage no comparison to observed data is made.

Firstly the relative sensitivity of the two parameters on both meshes is looked at. Figure 3.5 shows the impact of parameter variation on the total percentage inundation extent in the domain. It can clearly be seen from this that the bed friction has a far greater impact than the velocity diffusivity over the ranges tested.

a)

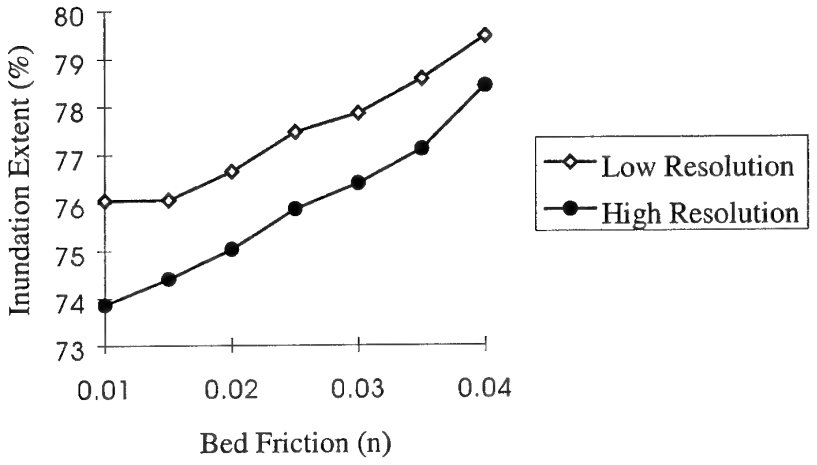

b)

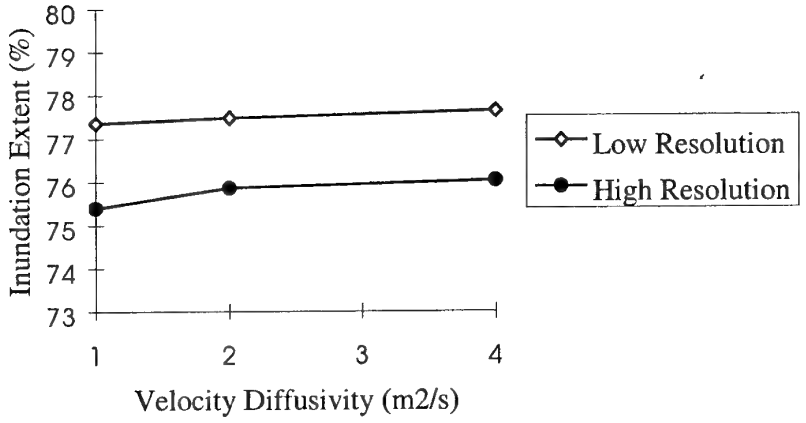

Figure 3-5 Inundation Extent change with (a) bed friction and (b) velocity diffusivity for both high and low resolution meshes.

Figure 3.6 shows the impact of both bed friction and velocity diffusivity on the water surface elevation at both gauge stations, Yankton and Gayville, for both mesh resolutions. The results in all cases show that the bed friction has a far greater influence on the water surface elevation than the velocity diffusivity.

a) Yankton

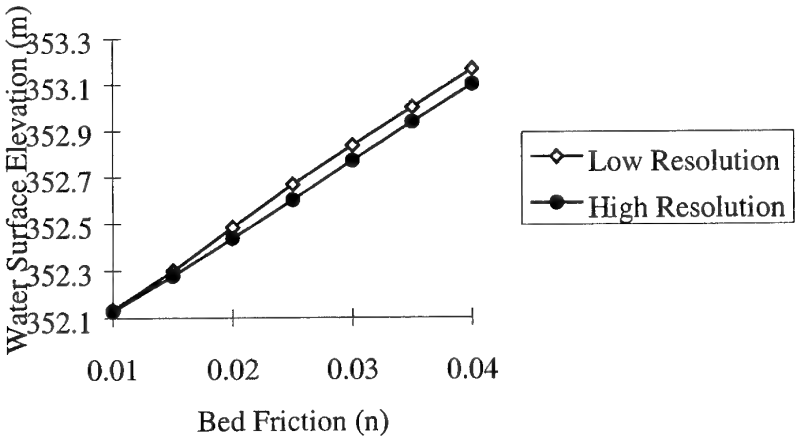

b) Gayville

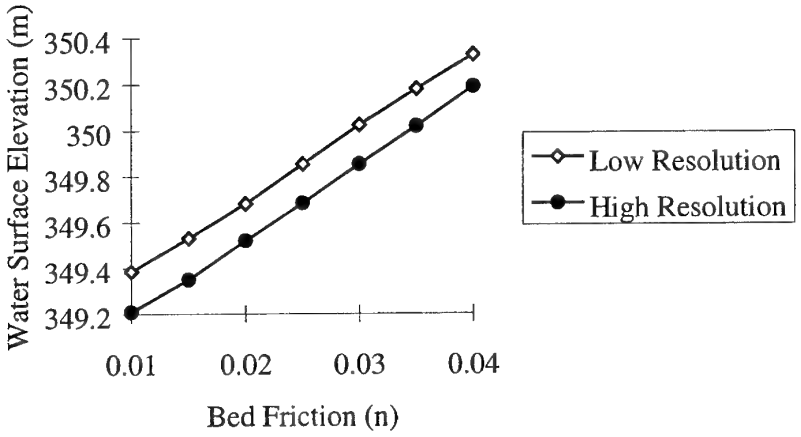

c) Yankton

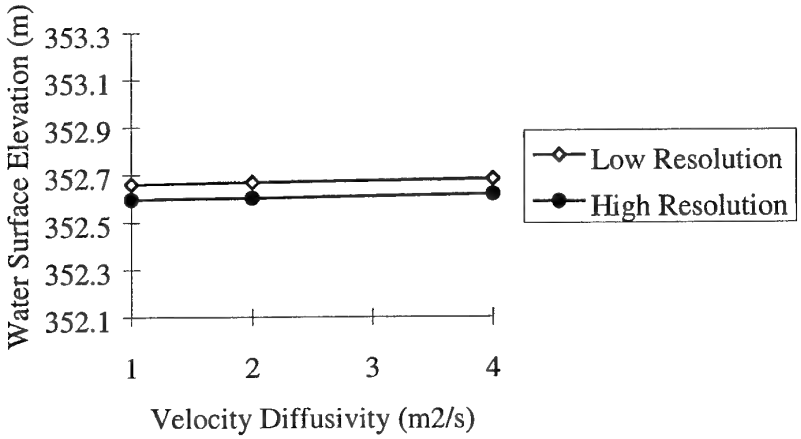

d) Gayville

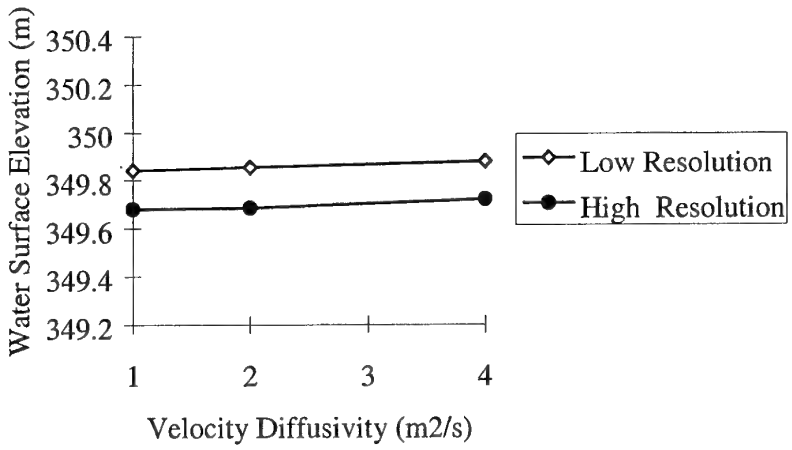

Figure 3-6 Sensitivity analysis plots for water surface against bed friction at (a) Yankton and (b) Gayville and against velocity diffusivity at (c) Yankton and (d) Gayville.

The impact of parameter variation on velocity at a point, in this case at Gayville, is shown in Figure 3.7. Bed friction is again dominant but the response is not linear.

a)

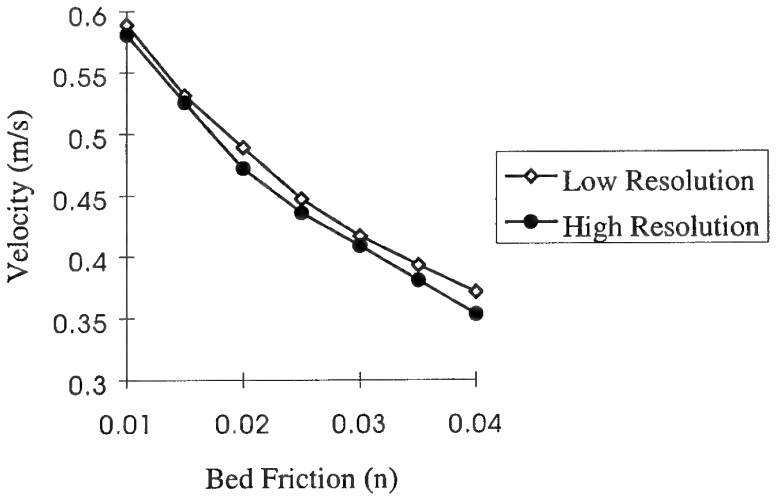

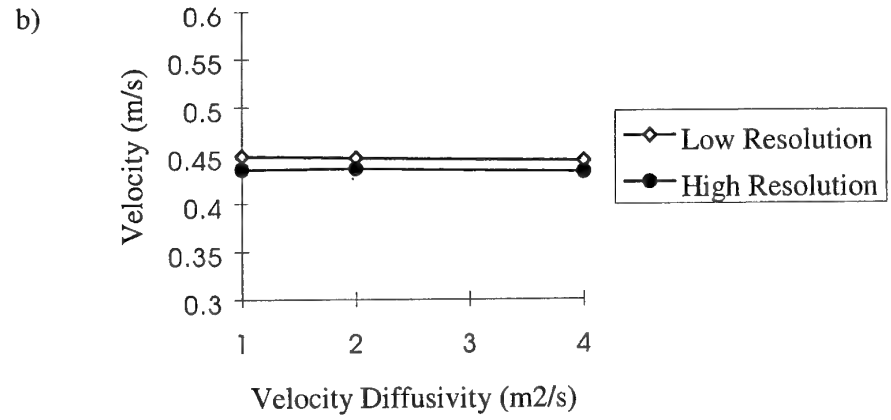

Figure 3-7 Change in velocity at Gayville as (a) bed friction and (b) velocity diffusivity varies for both high and low resolution meshes.

From the above three diagrams it is clear that the bed friction is clearly the most influential parameter having a far greater impact than velocity diffusivity on all the model results. The mesh resolution has a consistent impact on the model predictions. The greater the resolution of the mesh the lower the prediction for an equivalent parameter set for all model results. This is a slightly unusual result and shows that the model structure does have an important impact on the model predictions.

Having determined that the bed friction is by far the dominant parameter in the Missouri River model further analysis was carried varying only on this parameter. Using the argument of Troutman (1985), the velocity diffusivity can only introduce a small error into the results and varying it produces only small changes, hence it can reasonably be overlooked. The difference in velocity and water depth were calculated at all node points between the highest friction run (n = 0.04) and the lowest friction run (n = 0.01) on the Mesh 1. The results are then plotted up as a spatial plot of the domain.

The water depth difference plot (Figure 3.8a) clearly shows that along the thalweg the model behaviour is expected in that the water depth is greater with higher friction (positive difference values). On areas with very little or no water, such as sand banks in the channel or out of channel regions in the model, the behaviour is very much less marked with only very small changes being present, as would be expected. There are however areas in the model domain where the behaviour looks to be more complex and perhaps unexpected.

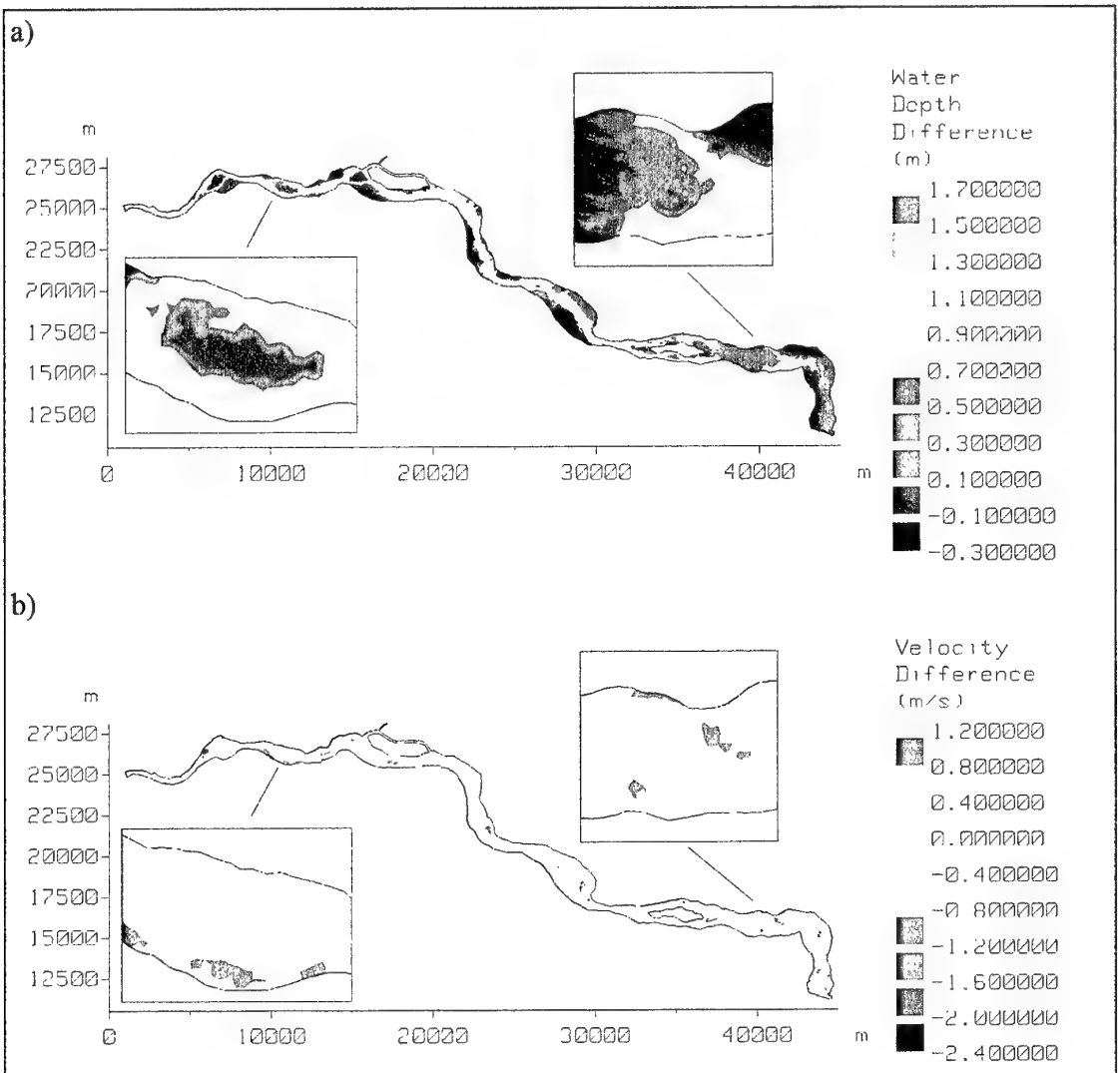

Figure 3-8 Difference surfaces created by subtracting the results of the lowest friction run (n=0.01) from the highest friction run (n=0.04) for (a) water depth and (b) velocity.

The velocity difference plot (Figure 3.8b) looks to more complex in structure than the water depth one. Along the thalweg the velocity is generally lower with the higher friction (negative difference values) but in the shallower regions the opposite is true. This is due to the water depth increase in these shallow areas facilitating an increase in velocity despite the increased bed friction. There are however many areas in the model where the behaviour is unexplained.

Further analysis of these plots has been carried out to find out more about the complex model behaviour at all the nodes. The nodal values of velocity difference, water depth difference, and the water depth for the low friction run were extracted from TELEMAC-2D results files. The velocity difference was then plotted against the two water depth variables mentioned. The results are of great interest (Figure 3.9) and show that unexpected model behaviour is much more frequent than anticipated.

Figure 3.9a shows the velocity difference plotted against the water depth in the low friction run and in this case, from the above discussion, it would be expected that at all nodes but those of very shallow depth the velocity difference should be negative. This is however clearly not the whole story. Although the majority of velocity differences are negative there are, across the whole depth spectrum, nodes that show the opposite behaviour. At very low (near zero) depths the majority of nodes do show an increase in velocity but this is not complete. The magnitude of the velocity differences seems to be greater at smallish depths (around 1m) possibly caused by bed friction having a greater influence on flow hydraulics at such depths than at greater depths. Although with the limited number of points at greater depths this could just be a random effect.

a)

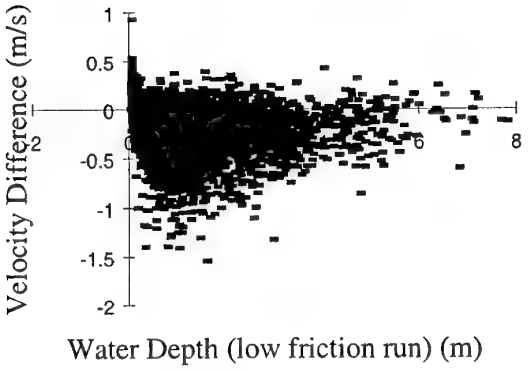

b)

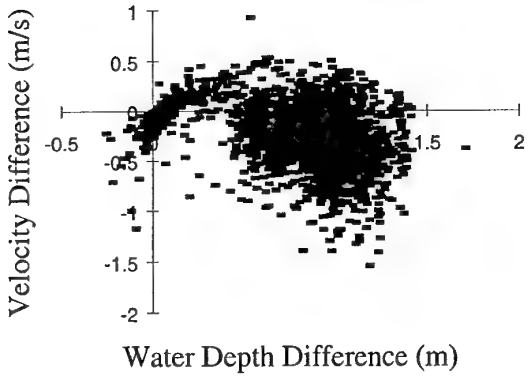

Figure 3-9 Sensitivity analysis plots showing results for all node points for differences between high and low friction runs for (a) velocity difference against water depth in the low friction run and (b) velocity difference against water depth difference.

Figure 3.9b shows the velocity difference against the water depth difference. The first point to note is that there are points that unexpectedly show a decrease in water depth

as friction increases. All these points also show a decrease in velocity. Between water depth changes of approximately 0 to 0.5m there is predominantly an increase in velocity as friction increases, probably corresponding to the nodes with shallow water depths initially. At greater water depth differences the majority of the behaviour is as expected, decreasing velocity as friction increases but there is a significant proportion of nodes revealing the opposite, though not to the same magnitude.

These results have shown the complexity of the model response to very simple changes in parameter values. Some of the unusual results can be explained by physical reasoning, others are perhaps artefacts generated by the model specification.

3.5.3 Conclusions of the sensitivity analysis

The sensitivity analysis has shown that the bed friction is by far the most influential parameter on all outputs in this model application. The strategy for calibrating the model must therefore be based on varying this parameter. At present the parameters are distributed evenly over the entire model domain but although this is perhaps simplistic there is no case, or data, to change them at the moment. The mesh resolution has a consistent influence on the model predictions showing the model structure is an important factor in the determining the model predictions. The sensitivity analysis also highlighted some strange and unexpected non-linear responses in some areas of the model domain.

4. Comparison of model predictions to observed data

4.1 Methods of Comparison

The data available for this study is stage data at two sites within the model domain which can be considered internal but 1-D and numerical. The satellite images are also internal but 2-D and numerical. The satellite imagery is therefore the more powerful validation data type. How well the observed and predicted data match shall be shown in the following sections and at the end this idea of strength of validation shall be revisited in the light of the results. Firstly however, the methods of model application used in this study and elsewhere are reviewed.

Usually when hydrological models are applied to actual scenarios a two stage process of model calibration and validation is carried out. Calibration is the process by which parameter values are varied within reasonable ranges until the differences between observed and computed values are minimised (Konikow and Bredehoeft, 1992). Theoretically speaking, physically-based models should not need calibrating. The estimation and application of physically realistic parameter values for the model should enable the model to perform well without any further manipulation. However, the numerous simplifications involved in modelling and problems in parameter estimation mean that such a notion is unrealistic. Calibration is therefore performed on virtually all physically based hydrologic models. Following the calibration phase the model must then be validated. In most cases the calibrated parameter values are used again on a different portion of the flow record to see if they enable a good match between observed and predicted variables. If they do, then the model and parameters are considered validated and can be used with confidence for prediction of future events. If not, then calibration and possibly some stage of model re-formulation must be undertaken until the model can be validated. It should be noted at this point that validation is used here to mean that a reasonable comparison is obtained between observed and predicted data rather than that the model has been shown to be an accurate representation of the system.

With this application of TELEMAC-2D, the highly structured methodology for calibration and validation outlined above is not entirely appropriate for several reasons:

- this study is for research of model behaviour,
- the number and variety of data sources make its application difficult,
- there is no need to produce a model capable of predicting future events at this stage,

The two processes are therefore not used as distinct entities in the following investigation. Instead a hybrid of the two forms was used enabling all benefits of the calibration-validation procedure to be accrued but also much more. The model was therefore run using a wide range of bed friction values over several sections of the flow record. This enabled the calibrated parameter values to be found for each comparison data set (2 internal stage gauges and possibly some areas on a satellite image). Cross comparison of parameter values and the assessment of errors when the model was calibrated onto one data source allowed an assessment of the model/parameter performance more complete and powerful than with the traditional calibration-validation procedure.

The time period being simulated for this comparison is around 6th June 1994 synchronous to the LANDSAT-TM satellite image of the area that will be used in section 4.3. The flow record around this date showed very little (<2%) variation in the data set. The simulation was therefore taken as a simple steady state computation, simplifying the analysis of results. All the following comparisons are therefore done on a single point in time basis, e.g. a single water level for each point in the domain for each parameter set.

4.2 Comparison of model prediction with internal stage data

Two internal gauges for water level are available for the reach of the Missouri River described in section 1. The gauges are at Yankton, 7.5 km down the reach, and Gayville, 21.5 km down the reach (see Table 3.1). Hourly stage records are available for these gauges.

The sensitivity of the model prediction of water depth at these two locations has been shown to be dependant predominantly on the bed friction parameter. This is the only parameter varied in the following analysis. Other parameters would have only minimal effect but increase complexity greatly. The sensitivity of water depth to friction is virtually linear at both internal gauge sites (Figure 4-1) and in the expected direction, i.e. water depth increasing as friction increases.

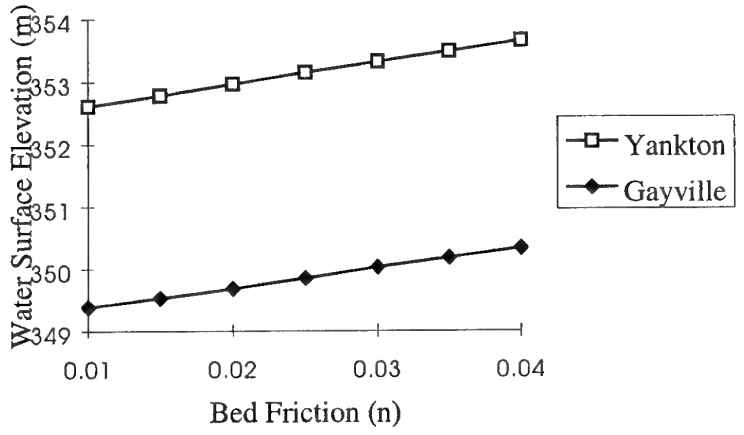

Figure 4-1 Linear sensitivity of water surface elevation to bed friction at the two gauge sites, Yankton and Gayville.

This finding allows the use of McCuen's (1973) linearized sensitivity equation but a simple regression equation is more useful for applying the results in this analysis and is therefore used here. Equations were produced for the model behaviour at both sites, Yankton and Gayville, relating the error in water level prediction to the bed friction (Manning's 'n') parameter. The equations, calculated using the statistical computing package MINITAB, can be written thus:

Yankton Error = -0.410 + 34.72 n
Gayville Error = -0.976 + 31.93 n

Alternatively they can relate the water depth to the bed friction thus:

Yankton Water Depth = 4.87 + 34.72 n
Gayville Water Depth = 2.91 + 31.93 n

The confidence in these regression lines is huge with tiny residuals (<0.015m) in all cases. These equations can therefore be used as a very powerful tool for estimating model predictions for 'n' values at which the model has not been run, although it should not be extrapolated beyond the range of 'n' values used to make the relationship (i.e. 0.01 to 0.04). At present this is only shown at two points but could perhaps be applied at every node.

It can easily be calculated from the above equations that the 'n' value to eliminate the error in water surface elevation at Yankton is 0.0118 whereas at Gayville it is 0.0306. The power of the above regression equations can now be utilised to calculate the error in the other observation whilst one is correct. Whilst the stage at Yankton is predicted correctly at Gayville the prediction is 0.60m too low. Reversing this, whilst Gayville is predicted correctly the prediction at Yankton is 0.65m too high. In percentage terms these errors are 18.26% and 10.96% of the expected water depth at the two points respectively.

Taking the value central to the above two estimates of Manning's 'n' should enable the approximate calculation of the joint minimum errors in the predictions. This value of 'n' is 0.0212 and produces an error at Yankton of 0.33m and at Gayville of -0.30m. Slight adjustment of 'n' could equalise these errors but would be irrelevant. These errors can be expressed again as percentages of the water depth such that the error at Yankton is 5.89% and at Gayville is 8.37%. Figure 4.2 shows a downstream section of the comparison between observed and predicted water surface values.

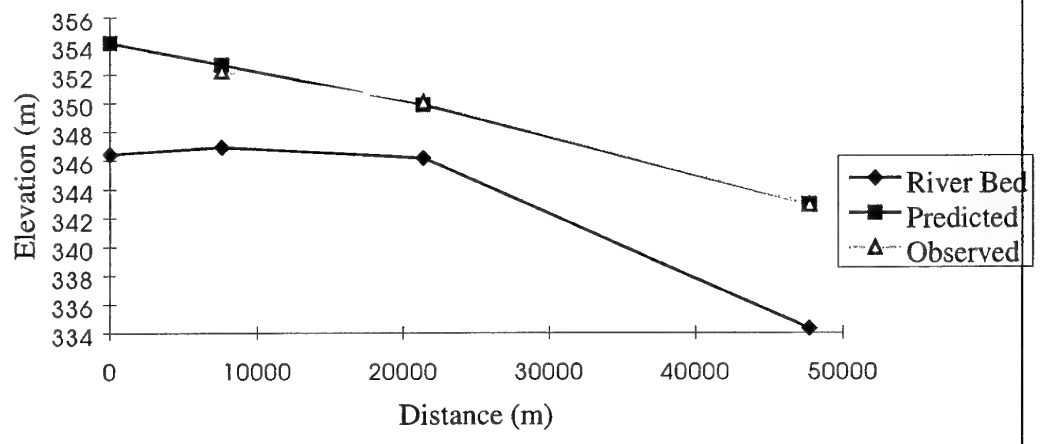

Figure 4-2 Downstream section of the reach showing the elevations of the river bed, observed water surface and predicted water surface (using a bed friction of n = 0.025) at the 4 gauges.

Interestingly the value of rate of change of the water surface (error term or water depth) is different at the two gauging stations. Thus a fixed change in the bed friction

produces a different change in the water surface elevation at the two stations. Investigation into how this type of behaviour occurs over the whole reach would be useful in determining more about model behaviour or what causes this phenomenon.

The comparison between observed an predicted stage values has shown that the model is capable of predicting this variable to about 0.3m at two sites simultaneously. This is a good result given the simplicity of the model set up. Given further work on the parameterization this could no doubt be reduced significantly.

4.3 Comparison of model inundation predictions with satellite imagery

Many types of satellite imagery have been used in studies of fluvial and coastal hydraulics. The wide coverage, ease of use and wealth of information contained in the images makes them ideal for many uses in this field. Redfern and Williams (1996) review the available sensors and their applications in (primarily coastal) hydraulics. Previously a lot of work has been carried out on the remote sensing of flood extent because of the immense hazard and mitigation costs on floodplain developments. Rango and Salomonson (1974) show that the areal extent of flooding can be mapped using near-infrared sensors on ERTS 1 (Earth Resources Technology Satellite - later renamed Landsat). More recently Imhoff *et al.* (1987) use SAR (Synthetic Aperture Radar) and Landsat MSS (Multispectral Scanner) for mapping flood extent and damage in Bangladesh. SAR has been shown to very accurate for flood boundary delineation by Biggin and Blythe (1996) on the River Thames in the UK. Satellite remote sensing of the 1993 floods on the Mississippi and Missouri Rivers in the USA with both SAR (Brackenridge *et al.*, 1994) and Landsat TM (Thematic Mapper) have further shown the potential of such methodologies.

Satellite data has also been used to measure flood stages as illustrated by Koblinsky *et al.* (1993) using the U.S. Navy's Geosat radar altimeter on the Amazon basin and Brackenridge *et al.* (1994) using SAR data and topographic maps on the Mississippi. Both methods have quite large errors associated with them at present.

Plumes of sediment rich water can also be identified as they have a higher reflectance than clear water in the visible region of the spectrum (Lillesand and Kiefer 1987). Brackenridge *et al.* (1994) use this factor to highlight levee breaches along the Mississippi River during the 1993 floods, the breaches acting as a sediment sources, and explain sediment deposition patterns. Other forms of pollution and thermal emissions can also be traced (Lillesand and Kiefer, 1987).

The availability of satellite imagery for the modelled reach of the Missouri River synchronous to the flow records has enabled several fundamental research objectives to be addressed. Data from satellite images is ideal for use with 2-D fluvial hydraulic models being of a scale commensurate to the model resolution and being widely spatially distributed. In this study such data has the potential to be used for:

- validation of inundation extent predictions,
- identification of regions of error,
- as calibration data,
- and for process validation.

Remotely sensed data has the potential to be used more widely in hydraulic modelling for topographic and physical parameterization (Bates *et al.*, 1997) but these are ongoing research themes.

Two sites at which to analyse model inundation predictions were chosen. These were selected specifically because of their complex bathymetry and topography, involving mud flats, permanent and temporary islands. The location of the two sites are shown on Figure 4-3. Side by side comparisons of the observed and predicted inundation are to be made using different friction values at both sites followed by an overlay showing the geo-referencing that can be done to the results.

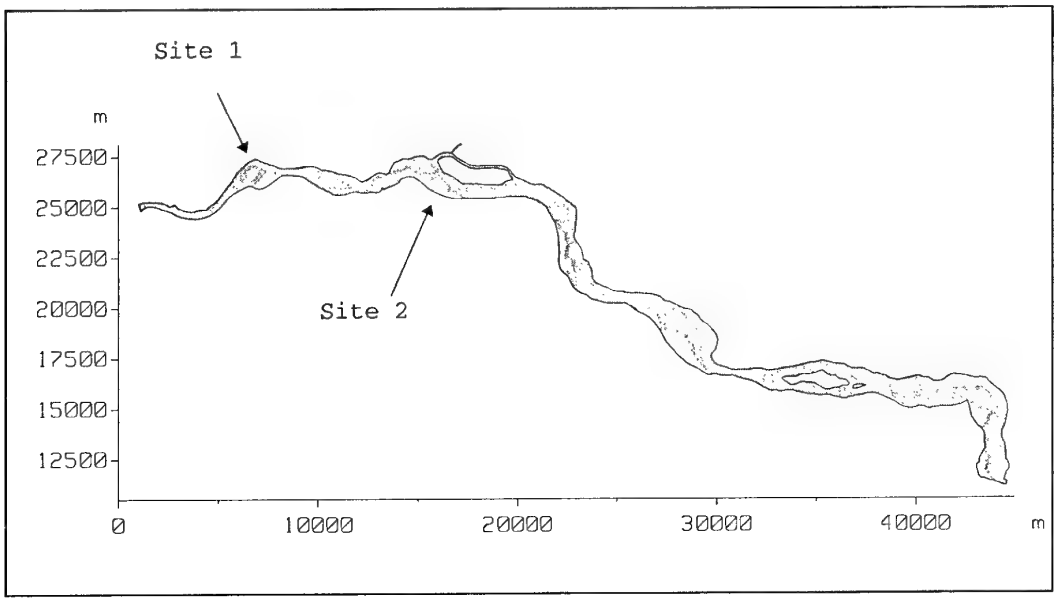

Figure 4-3: Locations of the two sites to be used in the comparison of model predictions with satellite imagery.

The side by side comparisons of the model predictions against the Landsat TM image, using bed friction values of 0.01, 0.02, 0.03 and 0.04, are shown in Figure 4-4 and Figure 4-5 for the two sites. These figures plot the satellite image against the predicted flow field boundary as this is the model result that can be directly compared to the image. From these it can be seen that the model predictions are generally good, producing a close spatial match against the observed data. This allows calibration of the model to be carried out with such data by varying bed friction until there is a close spatial match between observed and predicted. This variable behaviour is caused by the gradient of the topography around the water surface. If the topography has a shallow gradient then changes in the bed friction, changing the water depth, causes changes in the inundated areas. Where the topographic gradient is steeper then the same changes in water depth shall have virtually no impact on inundated area. A problem arises in this specific case, as far as calibrating the model on this data, because the topography above the water surface was only estimated from US Department of the Interior maps and is therefore probably not of the accuracy required to enable much confidence to be placed in the predictions of inundated area on islands.

Figure 4-4: Comparison of Landsat TM image and 4 alternative model predictions with different bed friction (Manning's 'n') values at site 1.

Figure 4-5: Comparison of Landsat TM image and 4 alternative model predictions with different bed friction (Manning's 'n') values at site 2.

By geo-referencing the model results and satellite image an overlay of the two can be made. An example of such is shown in Figure 4-6 for a section of this reach including site 2. This detailed comparison between observed and predicted flow field boundary enables problem areas to be pinpointed and further model development to proceed by further data collection or adjustments to the model in these areas.

Figure 4-6 An overlay of the model prediction of flow field boundary onto the Landsat TM image for a region around Goat Island (including site 2).

4.4 Summary

These first simulated flow conditions have shown both the excellent predictions of the 2-D hydraulic model and the utility of the data sources to validate its performance. The internal stage data was matched at single points but not so closely at both points simultaneously. The inundation extent was validated against the satellite images very well. Some areas showed up problems in the models bathymetry/topography. Given possible future refinements in the model set-up the internal stage data should be able to be matched simultaneously at both sites quite easily. Matching all the flow field boundaries may be more difficult given their dependence on the model bathymetry. This is however expected given the relative strength of the two validation types as discussed earlier.

5. Outline of the LISFLOOD model as a comparator model for river inundation and within channel flow process

To extend the above conclusions the TELEMAC-2D model was compared to an alternative simple inundation prediction code, LISFLOOD-FP, for a UK site where high resolution inundation extent data was available from SAR imagery. The LISLOOD-FP model is described in this section, whilst the high resolution data and model inter-comparison are described in Section 6. Finally, the impact of varying levels of bathymetric data provision and mesh resolution on the LISFLOOD-FP model is discussed in Section 7.

This LISFLOOD-FP model is described fully in Bates and De Roo (2000), but the salient points are reproduced here along with improvements made to the model subsequent to the original paper. Channel flow is handled using a one-dimensional approach that is capable of capturing the downstream propagation of a floodwave and the response of flow to free surface slope, which can be described in terms of continuity and momentum equations as:

$$\frac{\partial Q}{\partial x} + \frac{\partial A}{\partial t} = q \tag{5.1}$$

$$S_0 - \frac{n^2 P^{4/3} Q^2}{A^{10/3}} - \left[\frac{\partial h}{\partial x}\right] = 0 \tag{5.2}$$

Q is the volumetric flow rate in the channel, A the cross sectional area of the flow, q the flow into the channel from other sources (i.e. from the floodplain or possibly tributary channels), S_0 the down-slope of the bed, n Manning's coefficient of friction, P the wetted perimeter of the flow, and h the flow depth. In this case, the channel is assumed to be wide and shallow, so the wetted perimeter is approximated by the channel width. The term in brackets is the diffusion term, which forces the flow to respond to both the bed slope and the free surface slope, and can be switched on and off in the model, to enable both kinematic and diffusive wave approximations to be tested. With the diffusion term switched off, equation (5.2) can be solved for the flow Q in terms of the cross section A, and hence a partial differential equation in A is derived from equation (5.1). Usually, Q is chosen as the dependent variable (Chow, 1988, p 296), as it results in smaller relative errors in the estimation of discharge. For this model, however, we are primarily interested in water levels (which dictate the flood extent), so the cross sectional area A is used as the dependent variable. It also simplifies the inclusion of the diffusion term. An explicit non-linear finite difference system in A is then solved using the Newton-Raphson technique, rather than the linearised scheme used in the original model. The diffusion term can be included in an explicit fashion simply by modifying the bed slope, S_0, to include the depth gradient term. This approach can cause instability and the development of saw-tooth oscillations in the solution, but these are easily countered by the use of a smaller time step. If this is the case, the time steps for solving for channel and floodplain flows can be effectively de-coupled by using a number of sub-iterations for the channel flow.

A flow rate is imposed at the upstream end of the reach, which for the kinematic wave model is sufficient as a boundary condition, as wave effects can only propagate

downstream, and no backwater effects need to be taken into account. If the diffusion term is included, some downstream boundary condition is required to close the solution, as backwater effects are taken into account. This can either be a stage reading, or a zero free surface slope condition can be imposed, which leaves the depth at the downstream boundary free to vary, but prevents the solution developing a draw-down or draw-up curve. (This option will be referred to as a free downstream boundary condition.)

The channel parameters required to run the model are its width, bed slope, depth (for linking to floodplain flows) and Manning's n value. Width and depth are assumed to be uniform along the reach, their values assuming the average values taken from channel surveys. A uniform bed slope is calculated from the DEM (which is assumed to be too coarse to contain any explicit channel information), by linear regression along the line of the channel, which is defined by a series of vectors derived from large scale maps of the reach. It will be possible to derive such channel parameters from high resolution DEMs automatically. The remaining friction coefficient is left as a calibration parameter.

Floodplain flows are similarly described in terms of continuity and momentum equations, discretized over a grid of square cells, and two options exist in the model for the treatment of floodplain flows. Most simply, we can assume that the flow between two cells is simply a function of the free surface height difference between those cells (Estrela and Quintas, 1994):

$$\frac{dh^{i,j}}{dt} = \frac{Q_x^{i-1,j} - Q_x^{i,j} + Q_y^{i,j-1} - Q_y^{i,j}}{\Delta x \Delta y} \tag{5.3}$$

$$Q_x^{i,j} = \frac{h_{flow}^{5/3}}{n}\left(\frac{h^{i-1,j} - h^{i,j}}{\Delta x}\right)^{1/2} \Delta y \tag{5.4}$$

where $h^{i,j}$ is the water free surface height at the node (i,j), Δx and Δy are the cell dimensions, n is the Manning's friction coefficient for the floodplain, and Q_x and Q_y describe the volumetric flow rates between floodplain cells. Q_y is defined analagously to equation (5.4). The flow depth, h_{flow}, represents the depth through which water can flow between two cells, and is defined as the difference between the highest water free surface in the two cells and the highest bed elevation (this definition has been found to give sensible results for both wetting cells and for flows linking floodplain and channel cells.) The second option is to discretise the diffusive wave equation over the grid:

$$Q_x^{i,j} = \frac{\frac{h_{flow}^{5/3}}{n}\left(\frac{h^{i-1,j} - h^{i,j}}{\Delta x}\right)\Delta y}{\left(\left(\frac{h^{i-1,j} - h^{i,j}}{\Delta x}\right)^{1/2} + \left(\frac{h^{i,j-1} - h^{i,j+1}}{2\Delta y}\right)^{1/2}\right)^{1/4}} \tag{5.5}$$

The two approaches are subtly different: in the diffusive approach, the x,y components of the flow are linked, whereas in the cellular approach, the flow between

cells is solely a function of the component of free surface gradient in that direction. A possible criticism of the cellular approach is that it fails to reproduce some (intuitively correct) features of floodplain flows. For example, flow may not be parallel to the free surface gradient, depending on the orientation of the free surface slope and the model grid, but the two approaches agree when the slope is parallel to one of the grid axes. The differences between the two models can be derived analytically for a free surface slope of unit magnitude as a function of direction. The flow vectors differ in magnitude by a mean value of ~20% and in angle by ~10°. While these deviations may be partially compensated for in the friction calibration process (the cellular approximation predicts larger flows than the diffusive approximation), the effect on the bulk flow behaviour of the model is unclear, and so both approximations are tested in this study. Whichever approximation is adopted, an explicit scheme is used: floodplain flows are calculated first using equation (5.4 or 5.5), then the water depths on the floodplain are updated using (5.3).

Equations (5.4 or 5.5) are also used to calculate flows between floodplain and channel cells, allowing floodplain cells depths to be updated using (5.3) in response to flow from the channel. These flows are also used as the source term in (5.1), effecting the linkage of channel and floodplain flows. Thus only mass transfer between channel and floodplain is represented in the model , and this is assumed to be dependent only on relative water surface elevations. While this neglects effects such as channel-floodplain momentum transfer and the effects of advection and secondary circulation on mass transfer, it is the simplest approach to the coupling problem and should reproduce some of the behaviour of the real system.

Comparison of results from this simple code to those obtained from the TELEMAC-2D model have the potential to provide insights into both the physics of flood inundation and the nature of the modelling process. In particular, they may allow one to quantify the level of data provision necessary to achieve a particular prediction accuracy and allow one to more fully assess the ability of satellite derived inundation data to discriminate between competing model formulations.

6. Application of LISFLOOD using SAR data for validation

6.1 Test site and validation data

A 4 km long reach of the upper river Thames, UK, has been selected for comparison of the two models. For this site a 50m resolution, 25cm precision airphoto DEM is available, along with ground-surveyed channel cross sections. The DEM has been modified by the inclusion of a dyke (identified in maps of the reach) which runs for 500m along the north side of the channel at the upstream end of the reach. This was found necessary to constrain the flow in this region, and if omitted causes a gross overestimation of flood extent in the upstream part of the model. A gauging station is located at the upstream end of the reach, which can provide a boundary condition for the model. The floodplain environment is entirely agricultural, being mainly made up of meadow and rough pasture, which should make for an easier calibration problem with respect to floodplain friction. Bankful discharge is estimated at $40m^3s^{-1}$. A finite element mesh for the TELEMAC-2D model has been constructed using a streamline curvature dependent mesh generator (Horritt, 2000b) that ensures depth prediction

errors are independent of channel sinuosity. Element sizes vary from <50m near the channel to ~100m in the shoreline region. The mesh, along with the topography and channel for the LISFLOOD-FP model, is shown in figure 6.1. Steady flow is assumed throughout this study (peak inflow of 73 m^3s^{-1}), as given the short length of the reach and a typical kinematic wave propagation velocity (1.5 ms^{-1}), we would expect the reach to respond to changes in inflow in <1 hour. Even taking into account propagation times for the wetting front (measured at ~3 hours), this is still far quicker than significant changes in inflow (the hydrograph peak is ~40 hours in duration).

Validation data are also available in the form of satellite imagery (from the ERS-1 SAR sensor) of a 1-in-5 year flood event on the reach. This has been processed using a statistical active contour technique (Horritt, 1999, Horritt *et al.*, 2000) to extract the flood shoreline, which can then also be used to form a raster map of the inundation state. This technique has been found to delineate the shoreline with a mean location error of ~50m (Horritt *et al.*, 2000) when compared with airphoto data, which is probably adequate for this study, as it commensurate with the DEM resolution.

6.2 Model testing

Friction coefficients for the channel and floodplain remain unconstrained for this problem, and are therefore treated as calibration coefficients (Bates *et al.*, 1998, Horritt, 2000a). While this is likely to be a major source of model error, and will certainly cloud the issue of model comparison, the lack of alternative techniques for parameterising friction means that calibration is currently the only way forward. It also offers the opportunity of exploring the effects of friction parameterisation on the modelling strategies.

Firstly, we define the extent and dimensionality of the parameter space for the calibration problem. We assume only two friction classes, one for the channel and one for the floodplain, giving a two dimensional problem. Manning's n values for the channel range from 0.01 to 0.05, equivalent to values quoted for concrete lined straight channels and winding natural channels with vegetation and pools, respectively (Chow, 1988, p35). Values for the floodplain range from 0.02 to 0.10 or 0.12 (depending on the model used, see discussion below), equivalent to a surface somewhat smoother than pasture (n=0.035) to dense trees. This enables the full range of possible frictional values to be explored. For this reach (winding channel surrounded mainly by pasture with hedgerows), we would expect the optimum calibration to occur approximately in the centre of the parameter space, but as the friction calibration is also partly used to compensate for poorly represented processes in the model, the optimum may be shifted. Exploring the entire parameter space is a computationally intensive process, so a more pragmatic approach is adopted, instead aiming to explore only sparsely the full space, but focussing more attention on the area in the region of the optimum calibration.

Before calibration can be performed, we first also need to define some measure of fit between the observed and predicted flood extent, as it is this measure that will be optimised by the calibration process. We use an area based measure, the area correctly predicted as either wet or dry by the model, which is corrected for bias which may be introduced by the area occupied by the flood. For example, for a small flood in a large, mostly dry domain, even a relatively poor prediction of flood extent may give apparently good results in terms of the area correctly predicted by the model (i.e. the

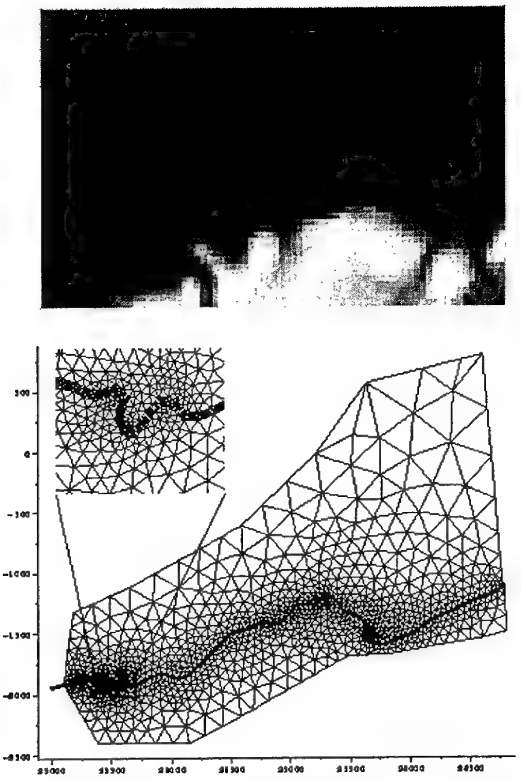

Figure 6.1: Finite element mesh and airphoto topography for the Thames text site.

large dry area). This can be rectified by ignoring an appropriate portion of the dry area, to make it equal in size to the flood. In this case, only 15.1% of the domain is flooded and 84.9% is dry, and so in the calculation of correct area, 69.8% (84.9-15.1%) is disregarded when the model predictions and satellite data are compared, in order to give approximately equal flooded/unflooded areas. Comparing results from the two models and the satellite data presents a little difficulty, due to the different scales and representations of the depth field used in the models. In this case, the results from the raster model are sampled onto a 12.5m grid (the resolution of the satellite data), and then can be compared directly on a pixel by pixel basis. The finite element results are also sampled onto a 12.5m grid, the depth field being linearly interpolated across each element. The treatment of shoreline regions requires special care: the water surface is extrapolated horizontally from the wet node(s) of a partially wet element and the shoreline defined as the intersection of the surface with the planar element topography. This means that the shoreline can lie within an element, rather than being confined to lying along element boundaries, which would be the case if the water surface was interpolated normally between wet and dry nodes.

The results of calibration for the LISFLOOD-FP model, using the kinematic wave approximation for channel flows and the cellular approximation over the floodplain, are summarised in table 6.1. The optimum calibration is (by chance) in the centre of the parameter space, occurring at friction values we would expect for this channel and floodplain environment. The model also shows more sensitivity to channel friction than floodplain friction, the measure of fit being >80% for all values of floodplain friction when Manning's n for the channel is set at 0.03. The results of the calibration are also shown in figure 6.2 as a contour plot of measure of fit over the parameter space, showing the optimum as a broad peak, and that the model has given a well behaved calibration problem. The best fit solution is shown in figure 6.3 with the SAR derived shoreline, showing that the model has predicted the inundation extent reasonably.

		n_{fl}				
		0.02	0.04	0.06	0.08	0.10
n_{ch}	0.01	65.2		65.8		65.8
	0.02		78.5	80.1	80.3	
	0.03	80.9	83.3	83.8	83.6	81.9
	0.04		79.9	78.3	72.1	
	0.05	79.0		65.5		45.1

Table 6.1: Calibration for LISFLOOD-FP model using the kinemtaic wave approximation for channel flow, showing fit with SAR data (% correct, corrected to remove bias) against floodplain friction (n_{fl}) and channel friction (n_{ch}).

Refinements in the model process representation may improve the results. Firstly, the diffusive approximation to floodplain flow is used, and the results displayed in figure 6.4. The results show now overall improvement in prediction accuracy (a maximum of ~80%), the model is slightly more sensitive to floodplain friction than before, and the optimum friction value has been shifted. Secondly, a diffusive wave approximation may be used in the channel. Figure 6.5 shows the water surface profiles for two simulations using the kinematic and diffusive wave approximations,

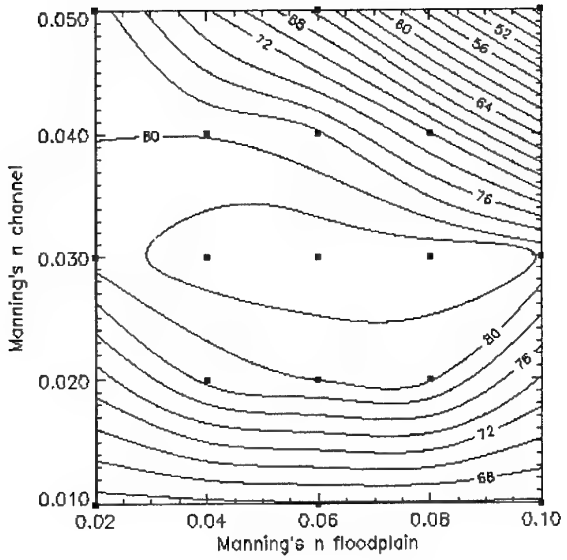

Figure 6.2: Results of calibration of the LISFLOOD-FP model using the kinematic wave approximation. The black squares correspond to points in the parameter space for which simulations were performed, the surface between points is found from inverse-square distance interpolation, and contoured using PV-Wave software. The contours are not meant to represent a realistic interpolation, but are merely a visualisation tool.

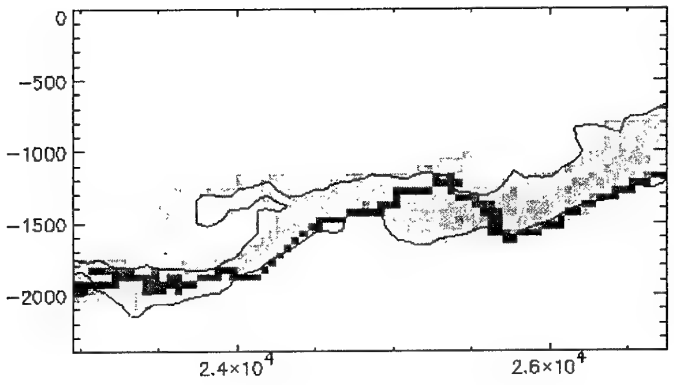

Figure 6.3: Best fit solution from the LISFLOOD-FP model using the kinematic wave approximation in the channel and the cellular model for floodplain flow.

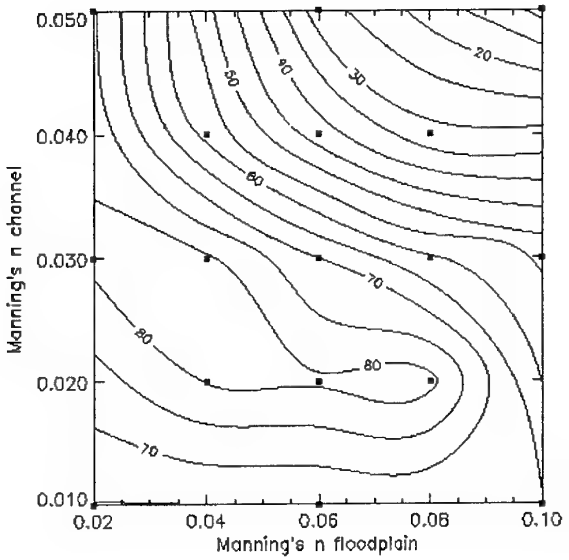

Figure 6.4: Results of calibration of the LISFLOOD-FP model using the kinematic wave approximation in the channel and the diffusive model for floodplain flow.

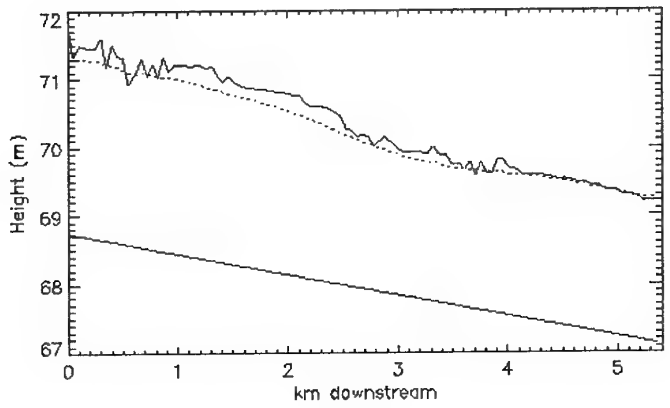

Figure 6.5: Water surface profiles along channel for kinematic (solid line) and diffusive (dotted line) wave models.

the kinematic model has predicted physically unrealistic variations in the free surface (induced by the linkage with floodplain flows), which are eliminated in the much smoother solution to the diffusive approximation. Nevertheless, both solutions have the same overall form, but with the diffusive approximation reducing water levels over the upstream half of the reach. A calibration of the diffusive channel flow scheme is given in table 6.2 and the resulting surface shown in figure 6.6. Figure 6.7 shows the best fit solution for the diffusive scheme. While the diffusive scheme has produced more realistic predictions of water depth over the channel, no overall improvement in model fit is made.

		n_{fl}				
		0.02	0.04	0.06	0.08	0.10
n_{ch}	0.01	66.2				
	0.02		74.2		76.1	77.2
	0.03			83.5	84.2	84.0
	0.04			84.7	84.7	83.7
	0.05		83.2	82.7	81.3	79.7

Table 6.2: Calibration for LISFLOOD-FP model using the diffusive wave approximation, showing fit with SAR data (% correct, corrected to remove bias) against floodplain friction (n_{fl}) and channel friction (n_{ch})

The results of the calibration of the TELEMAC-2D model are given in table 6.3 and shown in figure 6.8. The model fit covers a smaller range than for LISFLOOD, and the fit surface has a more complex form, although the higher sensitivity to channel friction is still present. The optimum fit is similar to that produced by the raster model using the kinematic wave approximation. The best TELEMAC-2D solution is shown in figure 6.9 with the SAR shoreline.

		n_{fl}					
		0.02	0.04	0.06	0.08	0.10	0.12
n_{ch}	0.01	75.5					
	0.02		79.0			79.7	
	0.03			79.8	80.2	81.2	81.4
	0.04			82.6	82.9	83.5	81.8
	0.05		82.4	82.3	82.4	82.6	
	0.06						82.0

Table 6.3: Calibration for TELEMAC-2D, showing fit with SAR data (% correct, corrected to remove bias) against floodplain friction (n_{fl}) and channel friction (n_{ch}).

The raster model seems to be capable of predicting inundation extent reasonably well, despite the rather crude assumptions of uniform bed slope, width, channel depth and friction. Refinements in the channel and floodplain flow representation have yielded no improvement in model results. It is interesting to note that the optimum channel friction gives a bankful discharge of 36 m^3s^{-1}, close to the Environment Agency estimate of 40m^3s^{-1}. Table 6.4 explores the model sensitivity to channel specification,

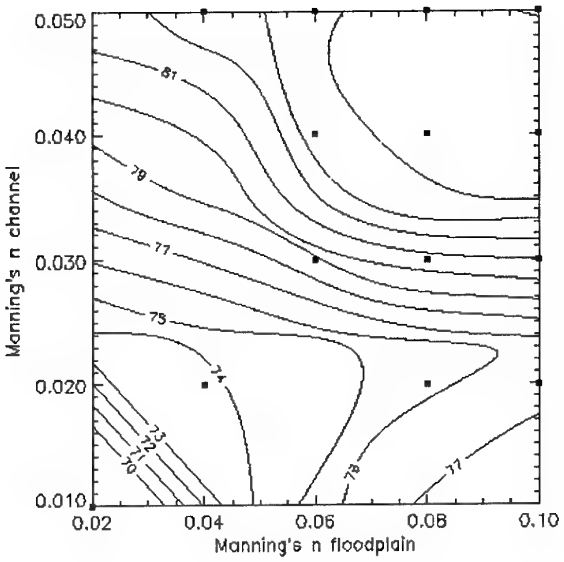

Figure 6.6: Calibration surface for the LISFLOOD-FP model using the diffusive wave approximation in the channel and the cellular model over the floodplain.

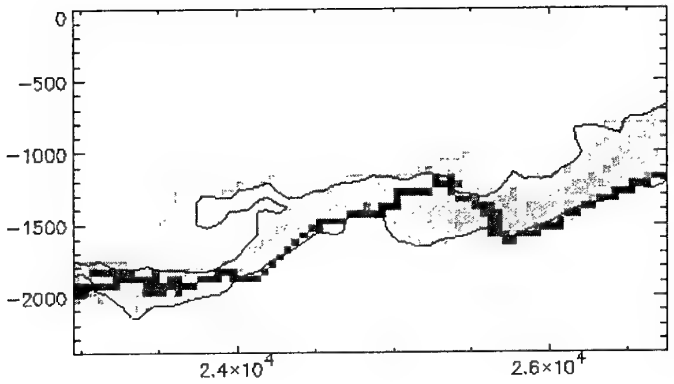

Figure 6.7: Best fit solution from the LISFLOOD-FP model using the diffusive wave approximation.

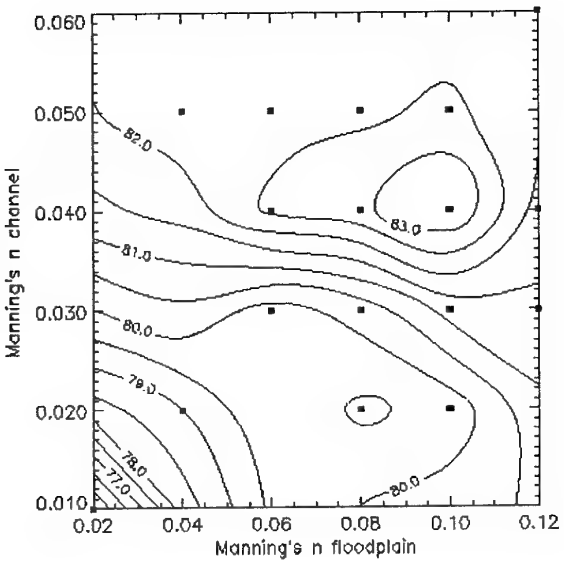

Figure 6.8: Calibration surface for the TELEMAC-2D model.

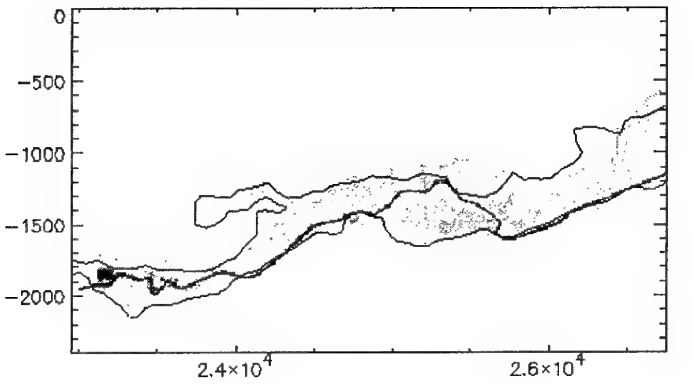

Figure 6.9: Best fit solution from the TELEMAC-2D model.

showing that it is still possible to achieve good results from the model even using the incorrect channel parameters, as long as the bankful discharge is approximately correct. This may be indicative of a certain insensitivity of model results to channel parameters, as long as the correct volume of water is being routed over the floodplain. However, it is unlikely that this result will hold for other reaches and other (possibly dynamic) events, and may be simply a peculiarity of this particular model and data set.

n_{ch}	Width (m)	Depth (m)	Bankful Discharge (m^3s^{-1})	Fit (%)
0.03	10	3.03	36.6	81.3
0.03	20	2.00	36.6	83.8
0.03	30	1.57	36.6	83.6
0.03	40	1.32	36.6	83.5
0.03	80	0.87	36.6	83.1
0.02	20	1.57	36.6	84.2
0.04	20	2.00	27.4	78.3
0.02	20	2.00	54.9	80.1

Table 6.4: LISFLOOD-FP model sensitivity to channel specification.

The numerical performance of the kinematic and diffusive raster models and the finite element scheme can also be compared in terms of mass balance errors and computational efficiency, given in table 6.5. Mass balance errors are calculated over each time step as:

$$Q_{error} = Q_{in} - Q_{out} - \frac{V_t - V_{t-1}}{\Delta t} \quad (6.1)$$

Q_{in} is the imposed upstream flowrate, Q_{out} is the model downstream flowrate, V_t and V_{t-1} are the volumes of water in the model domain at the current and previous time step and Δt is the model time step. The error can be thought of in terms of the volume lost or gained per second by the models. While it is difficult to come up with objective criteria of what constitute adequate mass conservation properties, the error figures given in table 6.5 are all probably less than the error in the inflow figure used to provide the upstream boundary condition. Given that the continuity equation is also liable to process representation errors (it neglects infiltration, runoff from bounding slopes, rainfall and evaporation), the mass balance errors found here probably have an insignificant effect on the predicted inundation extent. The time taken for 1000 iterations, along with numerical parameters for the models, are also given. The diffusive raster model required a 0.5s time step and 10 sub iterations for channel flows to achieve stability, compared to 1.0s and no extra channel sub-iterations for the kinematic scheme. The small time step used is a result of instabilities caused mainly by the linkage of channel and floodplain flows, the reduction of the time step and the use of sub-iterations being the easiest way around this problem without reformulation the explicit model. The raster models were coded in C++ and run on a 400Mhz Pentium II processor, and TELEMAC-2D in FORTRAN on a MIPS RISC 12000

300MHz processor in a Silicon Graphics Octane workstation. The figures show that the raster models have a considerable speed advantage over the finite element scheme, and all the models exhibit similar mass balance errors. Given the size of the domain (76 x 48 cell), the speed of the kinematic raster model is 3.5×10^{-6} s per cell per time step, 50 times faster than the PC-Raster coded model used in Bates and De Roo (2000), with a speed of 1.7×10^{-4} s per cell per time step.

Model	Time step (s)	Sub-iterations	Time per 1000 iterations (s)	Absolute Mass Balance Error (m^3s^{-1})
LISFLOOD-FP kinematic	1.0	1	12.8	0.05
LISFLOOD-FP diffusive	0.5	10	24.4	0.03
TELEMAC-2D	2.0	-	169	0.02

Table 6.5: Computational performance and mass balance errors for the three models

As a final test of the performance of both models, it is useful to compare their results with those from a crude predictor of flood extent, such as a planar water free surface height intersected with the DEM. This is a useful safeguard against the assumption that the hydraulic models are performing well, when, in fact, the problem of flood extent prediction may be trivial. The planar surface must be parameterised in terms of the heights at the upstream and downstream ends, and several techniques present themselves. The heights can be taken from water elevations in the channel, as measured at gauging stations, or from water elevations taken from the intersection between the SAR shoreline and the DEM. Both of these techniques may be prone to error caused by small local variations in water elevation in response to local hydraulic conditions, so a calibration methodology was instead adopted, whereby the upstream and downstream elevations of the planar surface are adjusted and the optimum fit with the SAR data sought. The results are given in figure 6.10, which shows a definite maximum (65%), and this best fit is shown in figure 6.11. The calibration surface for the planar predictor shows a greater sensitivity to downstream height as the flow is less constrained at the downstream end due to the lower transverse floodplain gradients. Given that using the unbiased measure of fit for classifying the whole of the floodplain as dry is 50%, the results of the hydraulic models (both raster and finite element) are a significant improvement over the planar free surface predictor. This is to be expected from the water surface profiles of figure 6.5, which show a considerable curvature in the surface, which will therefore be only poorly represented by a linear approximation.

6.3 Discussion

Both the raster model and the finite element scheme have performed reasonably when compared with the satellite imagery, but it is unclear whether further progress can be made at this stage. Errors in the SAR derived shoreline are of the order of 50m, according to Horritt *et al.*, 2000, who compared SAR derived flood shorelines against airphoto data over two 15km reaches of the river Thames. If this error is reproduced all along the shoreline, it is equivalent to misclassifying ~4% of the domain. This equates to an unbiased measure of fit of 87%, only slightly higher than the measures of fit we are obtaining with the inundation models tested here. This implies that we

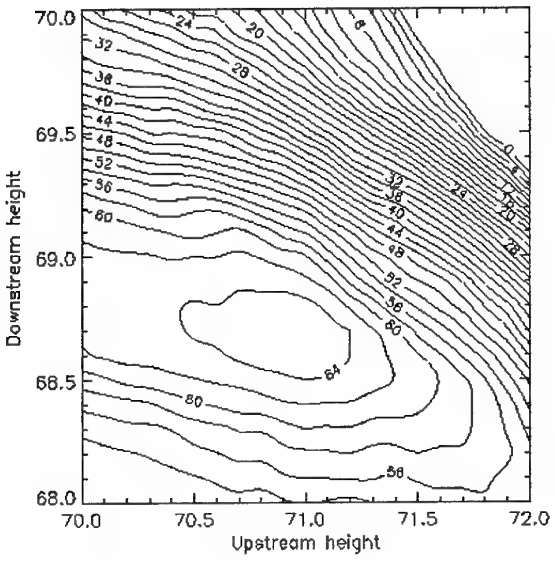

Figure 6.10: Calibration of planar free surface approximation, showing measure of fit as a function of upstream and downstream water elevations.

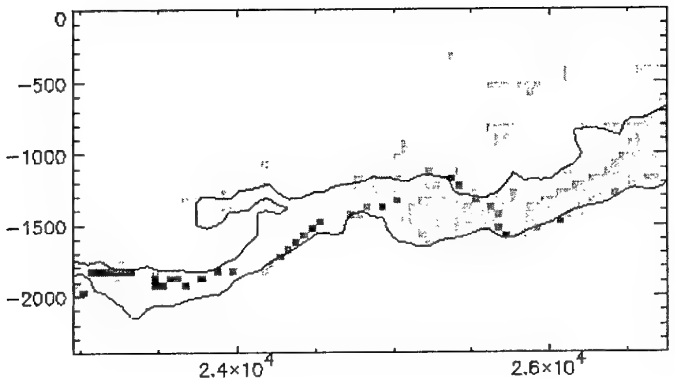

Figure 6.11: Best fit solution using the planar free surface approximation.

are achieving a similar measure of fit between model and SAR data as between SAR data and the real flood shoreline, and any further improvement in model performance is not possible with this data set. Both the raster and the finite element models achieve a similar measure of fit, but to distinguish further between them requires more precise validation data. It must be remembered that the optimum model formulation and calibration is not only dependent on the validation data, but the objective function used in the comparison with model predictions. The results of inappropriate process representation have thus been masked by uncertainty in the validation data, and at this level of uncertainty, a relatively crude process representation is enough to reproduce the observed inundation extent.

It should be stressed that this research has focussed on the use of hydraulic models as inundation predictors, and they have been tested as such against the SAR derived shoreline data. There will be only a weak link between inundation extent and floodplain and channel hydraulics, so this research only partially validates the hydraulic representations used in the model. This is demonstrated particularly well by the raster model's robustness with respect to channel specification. Very different channel widths and depths, with the constraint that they should approximately reproduce bankful discharge, can produce similar inundation patterns and measures of fit when compared to the SAR data, but with very different hydraulic conditions operating in the channel. This property is also demonstrated by the similarity of the raster models' predictions of flood extent using the kinematic and diffusive wave approximation. The unphysical variations in the free surface over the channel predicted by the kinematic model are not reflected in the flood shoreline, perhaps because these variations are in some sense damped out in the far flow field near the shoreline. This is encouraging in terms of inundation prediction, as it appears that in this case, as long as bankful discharge is approximately correct, the inundated area will also be approximately correct. Looking at the inverse problem, however, we see that inundation extent may give us very little information about channel flows.

This study has been limited to a single test site, and further applications to different sites are required to verify or disprove the results obtained here. There are a number of factors that may affect prediction accuracy when these modelling strategies are extended to other reaches. Inundation extent is very sensitive to topography, so the details of floodplain topography will affect the sensitivity to model formulation and calibration. Dynamic effects may also become important, especially over longer reaches. The kinematic wave velocity for the channel used here will be approximately 1.5 ms^{-1} (Chow, 1988, p284), and the surface wave celerity approximately 4.5 ms^{-1}, so kinematic effects should propagate along the 4km reach in ~1 hour. The maximum rate of change of the hydrograph for this event is 1.3 $m^3s^{-1}hr^{-1}$, so dynamic effects are unlikely to be important for this reach. Longer reaches will respond more slowly and with more complexity to the dynamic behaviour of the input hydrograph, and this may become a useful diagnostic tool for assessing model performance. For example, we have seen how the raster based model is fairly robust with respect to channel specification, as long as bankful discharge is reproduced reasonably well. Varying channel depth does, however, also affect kinematic and diffusive wave velocities, and so changing the channel properties may have much more of an effect for dynamic simulations than the steady state solutions developed here.

The application of hydraulic models to inundation prediction is still reliant on the calibration process, which tends to obscure model validation issues. The calibration process is model dependent: the TELEMAC-2D model produces the most complex calibration surface, while that for the LISFLOOD-FP model with kinematic approximation for channel flows is relatively simple, with the diffusive model somewhere in between. With all the models giving roughly the same level of fit at the optimum calibration (the optimum being model dependent), this is a point in favour of the simpler model. Given that currently we can only achieve closure in terms of friction parameterisation through a calibration procedure, the simpler calibration properties of the raster model are a definite advantage.

6.4 Conclusions

All the models tested here (raster kinematic, raster diffusive and finite element) have performed to a similar level of accuracy, classifying approximately 84% of the model domain correctly when compared to SAR derived shoreline data. However, the validation data used here is insufficiently accurate to distinguish between the model formulations, and the issue of model validation is further clouded by the calibration process necessary due to the lack of friction parameterisation data. The remotely sensed data has proved invaluable, however, in the calibration process, and has reduced the equifinality problem inherent in calibrating distributed models with point hydrometric data. Given the likely accuracy of the validation data, and the increasing complexity of the calibration process for models representing more complex processes, the simple raster based model using a kinematic wave approximation over the channel is the simplest (and fastest) model to use and adequate for inundation prediction over this reach.

7. The impact of varying levels of bathymetric data and mesh resolutions on the LISFLOOD-FP model predictions.

Section 6 established that even for best available data sets it may not be possible to discriminate between simple and complex hydraulic models. Given the relatively good performance of the LISFLOOD model, its computational efficiency and raster basis enable a more rigorous examination of data and resolution requirements than would have be possible with the TELEMAC-2D model. This work therefore has the potential to clarify a number of areas concerning topographic data provision for hydraulic models that can then be translated to more complex codes.

To achieve this, models of resolution varying from 10m to1000m were built for a 60km reach of the River Severn, UK and predictions compared with satellite SAR observations of inundated area and ground measurements of floodwave travel times, with a calibration strategy being used to determine channel friction coefficients. The optimum calibration was found to be stable with respect to changes in scale when the model was calibrated against the observed inundated area, the model reaching maximum performance at a resolution of 100m, after which no improvement was seen with increasing resolution. Projecting predicted water levels onto a high resolution DEM improved performance further, and a resolution of 500m proved adequate for predicting water levels. Predicted floodwave travel times were, however, strongly dependent on model resolution, and water storage in low lying floodplain areas near the channel was identified as an important mechanism affecting wave propagation

velocity. A near channel floodplain storage version of the LISFLOOD-FP model was shown to be much more stable with respect to changes in scale when the model was calibrated against floodwave travel times, and shown to represent the retardation of the floodwave caused by water storage near the channel. The LISFLOOD-FP model could not, in this instance, be calibrated to simultaneously give both acceptable travel times and inundated areas.

8. Future R&D opportunities

This project has sought to develop a suite of computational hydraulic models for high-resolution flow prediction at the reach scale (10-60km) that directly addresses potential COE Research and Development agendas. Specifically, we have:

- Developed a suite of models of varying complexity for long reach, high-resolution river flow prediction.
- Developed through GIS technologies the integration to remote sensing data sets capable of parameterizing such models and examined data assimilation, redundancy and scaling issues.
- Developed novel means of validating hydraulic models using newly available data sets from satellite and airborne sensing platforms.

Future opportunity: With the further advance of remote sensing technologies and high performance computing considerable potential now exists for computational hydraulic modelling at all scales up to and including the basin scale (100's of km). This has the potential to allow extension of the modelling techniques described in this report into the areas of:

Forecasting
- Real time forecasting
- Linkages to remote sensing driven snow-melt forecasting models
- Hydraulic impacts of climate and land use change

Design
- Soft engineering design in respect of land use, habitat specifications
- Development of maintenance schedules and impact assessments.

Management
- Linking hydrologic and hydraulic models for Integrated Basin Management
- Floodplain management and planning, including integration of model outputs with socio-economic data sets to identify at risk populations
- Wetland restoration and management

9. References

Baird, L. and Anderson, M.G. (1990). "Flood inundation modelling using MILHY", US Army European Research Office, Final Technical Report, DAJA 45-87-c-0053, Volume 1, 337pp.

Bates, P.D., Anderson, M.G., Baird, L. Walling, D.E. and Simm, D. (1992). "Modelling floodplain flows using a two-dimensional finite element model", *Earth Surface Processes and Landforms*, **17**, 575-588.

Bates, P.D., Anderson, M.G., Price, D.A., Hardy, R.J. and Smith, C.N. (1996). "Analysis and developments of hydraulic models for floodplain flows". In M.G. Anderson, D.E. Walling and P.D. Bates (eds), "*Floodplain processes*", John Wiley and Sons, Chichester, 215-254.

Bates, P.D., Horrit, M.S., Smith, C.N. and Mason, D. (1997) "Integrating remote sensing observations of flood hydrology and hydraulic modelling", *Hydrological Processes*, (in press).

Bates PD, Stewart MD, Siggers GB, Smith CN, Hervouet J-M and Sellin RJH. (1998). Internal and external validation of a two-dimensional finite element code for river flood simulations. *Proceedings of the Institute of Civil Engineers, Water, Maritime and Energy* **130**: 127-141.

Bates, P.D. and De Roo, A.P.J., (2000). A simple raster-based model for floodplain inundation. *Journal of Hydrology*, **236**, 54-77.

Bathurst, J.C. (1988). "Flow processes and data provision for channel flow models". In M.G. Anderson (ed), "*Modelling Geomorphological Systems*" John Wiley and Sons, Chichester, 127-152.

Beven, K. (1979) "A sensitivity analysis of the Penman-Montieth actual evapotranspiration estimates", *Journal of Hydrology*, **44**, 169-190.

Beven, K.J. (1993). "Prophesy, reality and uncertainty in distributed hydrological modelling", *Advances in Water Resources*, **16**, 41-51.

Biggin, D.S. and Blyth, K. (1996) "A comparison of ERS-1 satellite radar and aerial photography for river flood mapping", *Journal of the Chartered Institution of Water and Environmental Management*, **10(1)**, 59-64.

Brakenridge, G.R., Knpx, J.C., Paylor, E.D. II, and Magilligan, F.J. (1994) "Radar Remote Sensing Aids Study Of The Great Flood Of 1993", *EOS, Transactions, American Geophysical Union*, **75(45),** November 8th 1994, 521 and 526-527.

Brooks, A.N. and Hughes, T.J.R. (1982). "Streamline upwind/Petrov-Galerkin formulations for convection dominated flows with particular emphasis on the incompressible Navier-Stokes equations", *Computer Methods in Applied Mechanics and Engineering*, **32**, 199-259.

Chow VT. 1988. *Applied Hydrology*. McGraw-Hill: New York; 572pp.

Cooper, A.J. (1996). "TELEMAC-2D, version 3.0 Validation Document". *Report EDF HE-43/96/006/A*, 74pp.
Estrela T and Quintas L. 1994. Use of GIS in the modelling of flows on floodplains. In *2nd International conference on river flood hydraulics,* White HR and Watts J (eds), Wiley, Chichester; 177-189.

Hardy, R.J. (1997), Unpublished Ph.D thesis, University of Bristol.

Hervouet, J-M, Hubert, J-L, Janin, J-M, Lepeintre, F. and Peltier, E. (1994). "The computation of free surface flows with TELEMAC - An example of evolution towards hydroinformatics". *Report EDF-LNH HE-43/94/046/A,* 34pp.

Hervouet, J-M and Janin, J-M (1994). "Finite element algorithms for modelling flood propogation". In P. Molinaro and L. Natale (eds.), "*Modelling of Flood Propagation Over Initially Dry Areas*", American Society of Civil Engineers, New York, 102-113.

Hervouet, J-M. and Van Haren, L. (1995). "TELEMAC-2D Version 3.0 Principle Note". *Report EDF-LNH HE-43/94/052/B*, 90pp.

Hervouet, J-M. and Van Haren, L. (1996). "Recent advances In numerical methods for fluid flows". In M.G. Anderson, D.E. Walling and P.D. Bates (eds), "*Floodplain processes*", John Wiley and Sons, Chichester, 183-214.

Horritt MS. (1999). A statistical active contour model for SAR image segmentation. *Image and Vision Computing* **17**: 213-224.

Horritt MS. (2000a). Calibration and validation of a 2-dimensional finite element flood flow model using satellite radar imagery. *Water Resources Research,* **36**, 3279-3291.

Horritt MS. (2000b). Development of physically based meshes for two-dimensional models of meandering channel flow. *International Journal for Numerical Methods in Engineering* **47:** 2019-2037.

Horritt MS, Mason DC and Luckman AJ. (2000). Flood boundary delineation from synthetic aperture radar imagery using a statistical active contour technique. *International Journal of Remote Sensing*, **22**, 2489-2507.

Howes, S. and Anderson, M.G. (1988) "Computer Simulation In Geomorphology". In M.G. Anderson(ed), "*Modelling Geomorphological Systems*" John Wiley and Sons, Chichester, 421-440.

Imhoff, M.L., Vermillion, C., Story, M.H., Choudhury, A.M., Gafoor, A. and Polcyn, F. (1987) "Monsoon flood boundary delineation and damage asssessment using space borne imaging radar and landsat data", *Photogrammetric Engineering & Remote Sensing*, **53(4),** 405-413.

Koblinsky, C.J., Clarke, R.T., Brenner, A.C. and Frey, H. (1993) "Measurement of river level variations with satellite altimetry", *Water Resources Research*, **29(6),** 1839-1848.

Konikow, L.F. and Bredehoeft, J.D. (1992). "Ground-water models cannot be validated", *Advances in Water Resources*, **15**, 75-83.

Lane, S.N., Chandler, J.H. and Richards, K.S. (1994). "Developments in monitoring and modelling small-scale river bed topography", *Earth Surface Processes and Landforms*, **19**, 349-368.

LaVenue, M., Andrews, R.W. and RamaRao, B.S. (1989) "Groundwater travel time uncertainty analysis using sensitivity derivatives", *Water Resources Research*, **25(7),** 1551-1566.

Lillesand, T.M. and Kiefer, R.W. (1987). "*Remote sensing and image interpretation*", John Wiley and Sons, New York, 721pp.

Marchuk, G.I. (1975). "*Methods of numerical mathematics*". Springer-Verlag, New York 316pp.

McCuen R.H. (1973) "The Role Of Sensivity Analysis In Hydrologic Modelling", *Journal of Hydrology*, **18**, 37-53.

Norton, W.R., King I.P. and Orlob, G.T. (1973). "A finite element model for Lower Granite Reservoir: a report prepared for the U.S. Army Corps of Engineers, Walla Walla District, Washington.". Water Resources Engineers, Walnut Creek, California, 105pp.

Pinder G.F. and Gray, W.G. (1977). "*Finite element simulation in surface and subsurface hydrology*". Academic Press, New York, 295pp.

Piro, M. (1993). "RUBENS reference manual (version 2.0)". *Report EDF-LNH HE-45/93.02*, 65pp.

Price, D.A. (1997) "An integrated approach to modelling floodplain hydraulics, hydrology and nitrate chemistry", Unpublished Ph.D. thesis, University of Bristol, 242pp.

Rango, A. and Salomonson, V.V. (1974) "Regional Flood Mapping From Space", *Water Resources Research*, **10(3),** 473-484.

Redfern, H. and Williams, R.G. (1996) "Remote sensing: latest developments and uses", *Journal of the Chartered Institution of Water and Environmental Management*, **10(6),** 423-428.

Troutman, B.M. (1985) "Errors and parameter estimation in precipitation-runoff modelling 2. Case study", *Water Resources Research*, **21(8),** 1214-1222.

Younis, B.A. (1996). "Progress in turbulence modelling for open-channel flows". In M.G. Anderson, D.E. Walling and P.D. Bates (eds), "*Floodplain processes*", John Wiley and Sons, Chichester, 299-332.